

# Dimensional Stability of Grout-Type Materials Used as Connections for Prefabricated Bridge Elements

PUBLICATION NO. FHWA-HRT-16-008

MAY 2016



U.S. Department of Transportation  
**Federal Highway Administration**

Research, Development, and Technology  
Turner-Fairbank Highway Research Center  
6300 Georgetown Pike  
McLean, VA 22101-2296

## FOREWORD

The increasing use of accelerated bridge construction methodologies has led to widespread use of prefabricated bridge elements. These elements are commonly constructed offsite and assembled in the field through the use of field-cast grout connections. The materials used in these connections must provide superior performance to guarantee the proper functioning of the structure; however, it is not uncommon for these grouted connections to exhibit cracking and subsequently leakage either through the grout or at the interfaces with the prefabricated components. This cracking is recognized as being linked to the shrinkage that these grouts exhibit during the first days and weeks after casting. As part of the Federal Highway Administration's efforts to facilitate the use of accelerated construction technologies, the Structural Concrete Research Program has assessed grout shrinkage performance and developed recommendations for appropriate use of grouted connections. This report presents the dimensional stability results (with special focus on shrinkage) of a wide range of grout-type materials, providing the basis for a broader understanding of the shrinkage performance that an owner could anticipate experiencing with these materials. This report will be of interest to engineers, academics, researchers, and industry partners who are involved with the specification and use of field-deployed grouts.

Jonathan Porter  
Acting Director, Office of  
Infrastructure Research and  
Development

### Notice

This document is disseminated under the sponsorship of the U.S. Department of Transportation in the interest of information exchange. The U.S. Government assumes no liability for the use of the information contained in this document.

The U.S. Government does not endorse products or manufacturers. Trademarks or manufacturers' names appear in this report only because they are considered essential to the objective of the document.

### Quality Assurance Statement

The Federal Highway Administration (FHWA) provides high-quality information to serve Government, industry, and the public in a manner that promotes public understanding. Standards and policies are used to ensure and maximize the quality, objectivity, utility, and integrity of its information. FHWA periodically reviews quality issues and adjusts its programs and processes to ensure continuous quality improvement.

## TECHNICAL REPORT DOCUMENTATION PAGE

1. Report No. FHWA-HRT-16-008	2. Government Accession No.	3. Recipient's Catalog No.	
4. Title and Subtitle Dimensional Stability of Grout-Type Materials Used as Connections for Prefabricated Bridge Elements		5. Report Date May 2016	
		6. Performing Organization Code:	
7. Author(s) Igor De la Varga and Benjamin A. Graybeal		8. Performing Organization Report No.	
9. Performing Organization Name and Address Office of Infrastructure Research & Development Federal Highway Administration 6300 Georgetown Pike McLean, VA 22101-2296		10. Work Unit No.	
		11. Contract or Grant No.	
12. Sponsoring Agency Name and Address Office of Infrastructure Research & Development Federal Highway Administration 6300 Georgetown Pike McLean, VA 22101-2296		13. Type of Report and Period Covered 2013–2015	
		14. Sponsoring Agency Code	
15. Supplementary Notes The research discussed herein was completed at the Turner-Fairbank Highway Research Center. Portions of the work were completed by SES Group & Associates, LLC, under contract DTFH61-13-D-00007.			
16. Abstract The research presented in this report focuses on addressing performance concerns related to dimensional stability (primarily early age shrinkage) of 11 commercially available grout-type materials. Some of these grouts, especially those classified as “non-shrink grouts,” have been observed to display significant dimensional instability when deployed in connection details during bridge construction projects. The test methods used to evaluate dimensional stability are those described in the ASTM C1107 test method. After an initial evaluation, it was observed that the test methods used for evaluating dimensional stability described in this standard specification consider several parameters simultaneously (e.g., chemical expansion and shrinkage, autogenous and plastic shrinkage, etc.), thus providing a qualitative approach that is only useful for comparative purposes. To more completely assess this variety of parameters, volume changes were assessed from a fundamental point of view, measuring pure expansion/shrinkage deformations via test methods such as ASTM C157 and ASTM C1698. The results show that most of the grouts evaluated in this research seemed to perform well in terms of dimensional stability when tested in accordance with ASTM C1107. However, separate testing to specifically assess autogenous and drying deformations (shrinkage and expansion) demonstrated that ASTM C1107 is not necessarily an appropriate means to capture the full range of critical dimensional stability behaviors. Given the fact that most of the cement-based grouts commonly exhibit shrinkage, this research also included additional tests focused on the partial shrinkage mitigation by including internal curing through the use of prewetted lightweight aggregates. In summary, this research demonstrates the types of shrinkage performance that can be expected from these types of grouts, the shortcomings of the commonly used test methods, alternative test methods that may better demonstrate real world performance, and an innovative way of reducing part of the shrinkage observed in some of the grouts.			
17. Key Words Accelerated bridge construction, prefabricated bridge element, grout-type materials, dimensional stability, shrinkage, internal curing		18. Distribution Statement No restrictions. This document is available through the National Technical Information Service, Springfield, VA 22161. <a href="http://www.ntis.gov">http://www.ntis.gov</a>	
19. Security Classif. (of this report) Unclassified	20. Security Classif. (of this page) Unclassified	21. No. of Pages 70	22. Price N/A

# SI\* (MODERN METRIC) CONVERSION FACTORS

## APPROXIMATE CONVERSIONS TO SI UNITS

Symbol	When You Know	Multiply By	To Find	Symbol
<b>LENGTH</b>				
in	inches	25.4	millimeters	mm
ft	feet	0.305	meters	m
yd	yards	0.914	meters	m
mi	miles	1.61	kilometers	km
<b>AREA</b>				
in <sup>2</sup>	square inches	645.2	square millimeters	mm <sup>2</sup>
ft <sup>2</sup>	square feet	0.093	square meters	m <sup>2</sup>
yd <sup>2</sup>	square yard	0.836	square meters	m <sup>2</sup>
ac	acres	0.405	hectares	ha
mi <sup>2</sup>	square miles	2.59	square kilometers	km <sup>2</sup>
<b>VOLUME</b>				
fl oz	fluid ounces	29.57	milliliters	mL
gal	gallons	3.785	liters	L
ft <sup>3</sup>	cubic feet	0.028	cubic meters	m <sup>3</sup>
yd <sup>3</sup>	cubic yards	0.765	cubic meters	m <sup>3</sup>
NOTE: volumes greater than 1000 L shall be shown in m <sup>3</sup>				
<b>MASS</b>				
oz	ounces	28.35	grams	g
lb	pounds	0.454	kilograms	kg
T	short tons (2000 lb)	0.907	megagrams (or "metric ton")	Mg (or "t")
<b>TEMPERATURE (exact degrees)</b>				
°F	Fahrenheit	5 (F-32)/9 or (F-32)/1.8	Celsius	°C
<b>ILLUMINATION</b>				
fc	foot-candles	10.76	lux	lx
fl	foot-Lamberts	3.426	candela/m <sup>2</sup>	cd/m <sup>2</sup>
<b>FORCE and PRESSURE or STRESS</b>				
lbf	poundforce	4.45	newtons	N
lbf/in <sup>2</sup>	poundforce per square inch	6.89	kilopascals	kPa

## APPROXIMATE CONVERSIONS FROM SI UNITS

Symbol	When You Know	Multiply By	To Find	Symbol
<b>LENGTH</b>				
mm	millimeters	0.039	inches	in
m	meters	3.28	feet	ft
m	meters	1.09	yards	yd
km	kilometers	0.621	miles	mi
<b>AREA</b>				
mm <sup>2</sup>	square millimeters	0.0016	square inches	in <sup>2</sup>
m <sup>2</sup>	square meters	10.764	square feet	ft <sup>2</sup>
m <sup>2</sup>	square meters	1.195	square yards	yd <sup>2</sup>
ha	hectares	2.47	acres	ac
km <sup>2</sup>	square kilometers	0.386	square miles	mi <sup>2</sup>
<b>VOLUME</b>				
mL	milliliters	0.034	fluid ounces	fl oz
L	liters	0.264	gallons	gal
m <sup>3</sup>	cubic meters	35.314	cubic feet	ft <sup>3</sup>
m <sup>3</sup>	cubic meters	1.307	cubic yards	yd <sup>3</sup>
<b>MASS</b>				
g	grams	0.035	ounces	oz
kg	kilograms	2.202	pounds	lb
Mg (or "t")	megagrams (or "metric ton")	1.103	short tons (2000 lb)	T
<b>TEMPERATURE (exact degrees)</b>				
°C	Celsius	1.8C+32	Fahrenheit	°F
<b>ILLUMINATION</b>				
lx	lux	0.0929	foot-candles	fc
cd/m <sup>2</sup>	candela/m <sup>2</sup>	0.2919	foot-Lamberts	fl
<b>FORCE and PRESSURE or STRESS</b>				
N	newtons	0.225	poundforce	lbf
kPa	kilopascals	0.145	poundforce per square inch	lbf/in <sup>2</sup>

\*SI is the symbol for the International System of Units. Appropriate rounding should be made to comply with Section 4 of ASTM E380.  
(Revised March 2003)

## TABLE OF CONTENTS

<b>CHAPTER 1. INTRODUCTION, OBJECTIVES, AND APPROACH .....</b>	<b>1</b>
<b>INTRODUCTION .....</b>	<b>1</b>
<b>RESEARCH OBJECTIVES.....</b>	<b>1</b>
<b>RESEARCH APPROACH.....</b>	<b>2</b>
<b>RESEARCH SIGNIFICANCE.....</b>	<b>2</b>
<b>OUTLINE OF REPORT .....</b>	<b>3</b>
<b>CHAPTER 2. LITERATURE REVIEW .....</b>	<b>5</b>
<b>INTRODUCTION .....</b>	<b>5</b>
<b>PBES .....</b>	<b>5</b>
<b>GROUT-TYPE MATERIALS.....</b>	<b>6</b>
<b>PREVIOUS RESEARCH ON GROUT PERFORMANCE .....</b>	<b>7</b>
<b>IC TECHNOLOGY .....</b>	<b>7</b>
<b>CHAPTER 3. EXPERIMENTAL PROGRAM .....</b>	<b>11</b>
<b>INTRODUCTION .....</b>	<b>11</b>
<b>MATERIALS AND MIXING PROCEDURES .....</b>	<b>11</b>
<b>FRESH PROPERTIES.....</b>	<b>14</b>
Initial Workability.....	14
Air Content and Unit Weight.....	15
Set Time .....	16
<b>HARDENED PROPERTIES .....</b>	<b>17</b>
Compressive Strength .....	17
<b>CHEMICAL PROPERTIES .....</b>	<b>18</b>
Heat of Hydration .....	18
Chemical Shrinkage .....	19
<b>SHRINKAGE PERFORMANCE .....</b>	<b>20</b>
Shrinkage Performance Requirements According to ASTM C1107 .....	20
Autogenous and Drying Deformations .....	22
<b>IC APPROACH .....</b>	<b>23</b>
Introduction.....	23
Mixture Proportioning with IC .....	24
<b>CHAPTER 4. RESULTS AND DISCUSSION.....</b>	<b>27</b>
<b>INTRODUCTION .....</b>	<b>27</b>
<b>WORKABILITY AND COMPRESSIVE STRENGTH .....</b>	<b>27</b>
Discussion of the Results .....	29
<b>DIMENSIONAL STABILITY.....</b>	<b>30</b>
Grouts Reactivity .....	30
Dimensional Stability According to ASTM C1107.....	32
Autogenous and Drying Deformations .....	34
Long-Term Sealed and Drying Deformations (ASTM C157).....	37
Preliminary Dimensional Stability Conclusions.....	41
Appropriateness of ASTM C1107 Tests Methods to Evaluate Dimensional Stability.....	41
<b>IC TECHNOLOGY .....</b>	<b>42</b>

Chemical Shrinkage for IC Design .....	42
Autogenous and Drying Deformations with IC .....	43
Compressive Strength with IC .....	46
Additional Cost to Include IC .....	46
<b>CHAPTER 5. CONCLUSIONS AND RECOMMENDATIONS .....</b>	<b>47</b>
<b>CONCLUSIONS AND RECOMMENDATIONS.....</b>	<b>47</b>
<b>ONGOING AND FUTURE RESEARCH .....</b>	<b>49</b>
<b>APPENDIX A. MANUFACTURER REPORTED GROUT PERFORMANCE</b>	
<b>INFORMATION.....</b>	<b>51</b>
<b>ACKNOWLEDGMENTS .....</b>	<b>57</b>
<b>REFERENCES.....</b>	<b>58</b>

## LIST OF FIGURES

Figure 1. Photo. Casting of a grout-type material in the connections between PBEs .....	6
Figure 2. Illustration. The differences between external curing and IC .....	8
Figure 3. Equation. Amount of IC water needed based on the chemical shrinkage occurring in the sample .....	8
Figure 4. Photo. Mixing M2 grout using a drill and a paddle.....	14
Figure 5. Photo. Flow table test as per ASTM C1437, including accessories to run the test (left) and grout spread (right).....	15
Figure 6. Photo. Air content and unit weight.....	16
Figure 7. Photo. Loading apparatus and penetration needles .....	17
Figure 8. Graph. Typical setting time data plot indicating initial and final set times.....	17
Figure 9. Photo. Compressive strength cube specimens (left) and cube specimen after test via ASTM C109 (right).....	18
Figure 10. Photo. Isothermal calorimeter and sample specimens via ASTM C1679.....	19
Figure 11. Photo. Chemical shrinkage testing via ASTM C1608.....	20
Figure 12. Photo. Modified ASTM C827 setup (left) and change length in a hardened specimen with ASTM C1090 (right) .....	21
Figure 13. Illustration. The apparatus for early change in height adapted from ASTM C827.....	22
Figure 14. Photo. ASTM C1698 tubes setup (top) and sealed and drying ASTM C157 specimens (bottom).....	23
Figure 15. Photo. Images taken in G4 dry samples: cross-polarized light thin section micrograph with yellow arrows showing non-reactive sand particles (top left); plane- polarized light of the same thin section micrograph with red and green arrows showing cement and fly-ash particles, respectively (top right); SEM image with orange arrow showing a silica fume particle (bottom left); and energy-dispersive X-ray spectroscopic analysis confirming the siliceous nature of the silica fume particle (bottom right).....	25
Figure 16. Graph. Heat flow during the first hours of reaction: no repair materials (low heat) (top) and repair materials (high heat) (bottom).....	31
Figure 17. Graph. Change in height at early ages according to a modified version of ASTM C827.....	33
Figure 18. Graph. Autogenous (sealed) shrinkage as a function of time via ASTM C1698.....	35
Figure 19. Photo. Representative SEM images of the G3 grout: predominant ettringite (needle-shape) phase formation in the matrix at 2 d of hydration .....	37
Figure 20. Graph. Comparison of autogenous shrinkage results obtained using the ASTM C1698 corrugated tubes and the ASTM C157 sealed specimens .....	38
Figure 21. Graph. Long-term autogenous (sealed) shrinkage as a function of time.....	39
Figure 22. Graph. Long-term drying shrinkage as a function of time .....	40
Figure 23. Graph. Chemical shrinkage as a function of time of two of the cement-based grouts.....	43
Figure 24. Graph. Effect of IC on the autogenous shrinkage .....	44
Figure 25. Graph. Effect of IC on the long-term autogenous (sealed) shrinkage (top) and long-term drying shrinkage (bottom) as a function of time.....	45

## LIST OF TABLES

Table 1. Grout-type materials used in the present study.....	12
Table 2. Mixing information of each of the grout-type materials.....	13
Table 3. Mixture proportions of the internally cured cement-based grouts.....	26
Table 4. Flow measurements using ASTM C1437 methods, set time, fresh air content, and unit weight .....	28
Table 5. Compressive strength results for grout cubes.....	29
Table 6. Minimum compressive strength for 2-inch (51-mm) cubes according to ASTM C1107.....	29
Table 7. Height change requirements according to ASTM C1107.....	32
Table 8. Height change of hardened grouts via ASTM C1090 test.....	34
Table 9. Effect of IC on the compressive strength.....	46
Table 10. Cement-based grouts.....	52
Table 11. Repair materials .....	53
Table 12. Epoxy-based grouts.....	54
Table 13. Ultra-high performance concrete .....	55



## LIST OF ABBREVIATIONS

ABC	accelerated bridge construction
IC	internal curing
LWA	lightweight aggregate
PBE	prefabricated bridge element
PBES	prefabricated bridge elements and systems
RH	relative humidity
SAP	superabsorbent polymer
SEM	scanning electron microscope
UHPC	ultra-high performance concrete
w/b	water-to-binder ratio
w/c	water-to-cement ratio
w/s	water-to-solids ratio



## CHAPTER 1. INTRODUCTION, OBJECTIVES, AND APPROACH

### INTRODUCTION

Accelerated bridge construction (ABC) consists of innovative bridge construction methods that are used in a safe and cost-effective manner to minimize the inconveniences to the travelling public while delivering a superior finished product. This technology has become common over the last two decades in the United States, and many States are considering ABC on more typical projects.

The use of prefabricated bridge elements (PBEs) facilitates ABC. These elements are typically produced in a controlled environment that facilitates high production quality. The most critical field construction process for prefabricated subassemblies is the completion of the connections between elements. In general, connections must be robust, durable, and efficient. One common connection method involves the use of field-cast concretes or grouts in the interstitial spaces between the prefabricated components. As would be expected, some PBE connection details have been linked to constructability and serviceability problems within the deployed systems. Many times these issues have been attributed to less-than-desirable performance of the field-cast grouts that can be used in the connections.

Grout-type materials, especially cement-based grouts, can provide ease of placement as well as rapid strength development when used to connect PBEs. However, they have also shown dimensional instability due to the rapid rate of (inherent) shrinkage and the presence of expansive agents to try to counteract most of that shrinkage. While the ASTM C1107 *Standard Specification for Non-Shrink Packaged Dry, Hydraulic-Cement Grout* test method describes how cement-based grouts are to be tested, this specification focuses on ensuring that the materials achieve a minimum strength and that the expansion achieved is below a maximum limit.<sup>(1)</sup> However, the specification lacks a clear presentation of shrinkage limits and does not speak to potential incompatibilities with the surrounding materials (i.e., prefabricated concrete substrate) that can have negative effects on the performance of the material. This research investigated the dimensional stability performance of a variety of different grout-type material categories that may be used in concrete infrastructure connections.

### RESEARCH OBJECTIVES

Grout-type materials have been extensively used in the construction industry. Their performance in terms of high workability and rapid strength development is well known and accepted by the end-users. Different types are currently available (e.g., cement-based, epoxy-based, etc.). However, rapid strength gain typically leads to rapid volume changes (e.g., expansion and/or contraction), especially in cement-based grouts, which are the most commonly used type of grout. In fact, there have been concerns about the lack of dimensional stability for this type of material. The main objective of the research effort reported herein was to better understand how these materials perform in terms of dimensional stability, especially at early ages, for their use in connections between prefabricated concrete elements. Once the dimensional stability was evaluated, means to partially mitigate most of the volume changes (especially shrinkage) were investigated. While one strategy consisted of providing internal curing (IC) through the use of

prewetted lightweight aggregates (LWAs), other non-traditional grouts, such as an ultra-high performance concrete (UHPC), were also investigated as potential strategies to enhance the dimensional stability of grout-type materials.

In summary, the goals of the overall report are as follows:

1. Assess the dimensional stability of common grout-type materials using standardized tests.
2. Discuss the appropriateness of existing dimensional stability test methods.
3. Introduce cost-effective shrinkage mitigation strategies. This is done by: (1) laying the groundwork for including IC in cement-based grouts and (2) investigating the dimensional stability performance of a UHPC.

## **RESEARCH APPROACH**

The research described in this report mainly focuses on the evaluation of the dimensional stability of commercially used grout-type materials that can potentially be used for connecting prefabricated concrete bridge elements. A selection of 11 different materials was made, including cementitious-based, epoxy-based, and magnesium phosphate-based grouts. A UHPC was also included in the research. Following the guidelines described in the ASTM C1107 test method, the grout performance in terms of initial fresh workability, compressive strength, and dimensional stability was assessed.<sup>(1)</sup> However, the test methods used for evaluating dimensional stability described in this standard specification have the inconvenience of considering several parameters simultaneously (e.g., thermal expansion, chemical expansion, chemical shrinkage, autogenous shrinkage, plastic shrinkage, settlement, etc.), thus providing a qualitative approach that is only useful for comparative purposes. To more completely assess this variety of parameters, volume changes must be assessed from a fundamental point of view by measuring pure expansion/shrinkage deformations. As such, additional tests to evaluate the dimensional stability of the grouts were carried out. These are described in ASTM C157, *Standard Test Method for Length Change of Hardened Hydraulic-Cement Mortar and Concrete*, and ASTM C1698, *Standard Test Method for Autogenous Strain of Cement Paste and Mortar*, test methods.<sup>(2,3)</sup> Other standardized tests were used in order to further characterize these materials. Finally, and given the fact that these grouts commonly exhibit shrinkage, this research also included additional tests focused on partial shrinkage mitigation by including IC in some of the cement-based grouts.

## **RESEARCH SIGNIFICANCE**

While the use of grout-type materials as connections between prefabricated concrete elements in bridges has been shown as a promising technique to facilitate ABC, the fact that they are designed with a low water-to-solids ratio (w/s) makes them prone to early-age shrinkage. Shrinkage under restraint can cause the development of tensile stresses within the grout, leading to premature cracking when the tensile strength of the material is still low, or can cause stresses at the interface leading to loss of bond between the grout and the concrete substrate. In this report, several types of commonly used prepackaged grouts were selected for assessment of their dimensional stability at both early and later ages. In some of the cementitious grouts, the

inclusion of IC through the addition of prewetted fine LWAs was evaluated. The IC technology in concrete has been broadly studied within the last decade, and its implementation in the concrete mixture design procedure is well defined at this point. In this study, IC is included in cement-based grouts, and the challenges encountered to do so are discussed. This method is proposed to improve curing conditions, since most of the grouts are poured in either sealed locations or points of difficult access for providing external (or conventional) curing. The results and conclusions are expected to provide guidance to designers and end-users in selecting the right grout-type material for use in connections between prefabricated concrete elements in bridges and other concrete structures.

## **OUTLINE OF REPORT**

The report is divided into five chapters and an appendix. Chapters 1 and 2 provide an introduction and literature review. Chapter 3 presents a detailed description of the experimental program followed in the study. Chapter 4 presents the results and an in-depth discussion of the results. Finally, chapter 5 provides the main conclusions and recommendations taken from the study. An appendix is also included that contains some of the main material properties taken from the manufacturers' product data sheets.



## CHAPTER 2. LITERATURE REVIEW

### INTRODUCTION

ABC is becoming more popular in the United States due to the advantages obtained in terms of safety, cost-effective construction, and congestion mitigation. The use of prefabricated concrete elements is a key part of ABC; however, the field-casting of the connections between these elements tends to be a critical and challenging part of making the overall system work successfully. The connections are typically made with grout-type materials, frequently cement-based grouts. The performance of these materials is crucial for the serviceability of the whole structure. Consequently, considerable research on how these materials behave has been done during the last decades. However, recent research shows the wide range of performance that can be obtained from grouts, as well as the propensity of the materials to undergo volumetric deformations (i.e., expansion and/or contraction). The main objective of this chapter is to provide an overview of the concepts of: (1) prefabricated bridge elements and systems (PBES), (2) grout-type materials and their general properties, (3) previous research performed on grout-type materials, and (4) the emerging use of IC technology in concrete materials.

### PBES

ABC has become common for both new and replacement bridge construction. ABC was developed due to the need to provide a fast and efficient manner to construct bridges without causing too much disruption to the facility. ABC uses innovative planning, materials, design, and methods that provide a faster and safer way to construct a bridge. ABC commonly uses PBEs that are built offsite and includes features that reduce the onsite construction time and mobility impact time that occur from conventional construction methods. Because these structural components are built off the critical path and produced under controlled environmental conditions, there are improvements in the product quality and the component long-term durability. ABC has been growing in prevalence around in the United States for about 20 years. Early projects focused on specific prefabricated elements such as bridge decks. More recently, ABC projects that use PBES have spread to all bridge elements.<sup>(4-6)</sup> The use of PBES in ABC has shown many benefits, including improved safety and working conditions for workers, reduced impact to users, improved quality of delivered product, and reduced cost to society in general. A photographic example of one type of PBE connection being completed through the casting of the grout is shown in figure 1.



**Figure 1. Photo. Casting of a grout-type material in the connections between PBEs.**

## **GROUT-TYPE MATERIALS**

Grout-type materials are widely used in the construction industry for different applications such as joint sealing, flooring, and structural repair, among others. (See references 7 through 13.) The most common grout type is based on cement or cementitious materials. It is generally a mixture of cement, sand, water, and powder chemical admixtures, and it is commonly referred to as non-shrink cementitious grout. Other types are also available, such as epoxy-based, fly-ash-based, and magnesium phosphate-based grouts, to name just a few. Grout-type materials are normally proprietary materials that are prepackaged and ready to mix on site.

As previously mentioned, one common use for grouts is in ABC within connections between prefabricated bridge structural elements.<sup>(6)</sup> These prefabricated structural components are produced under controlled environmental conditions, thus improving the quality of the product. Non-shrink cementitious grouts are most often used to easily and efficiently provide a connection between these precast concrete elements. Other types of grout may be acceptable for precast connections, but they are typically more expensive than cementitious grouts and may introduce the need for non-standard considerations on the part of the designer. Typically, the field casting of the connections is a labor-intensive, critical part of the overall long-term performance of the system. This is the reason why grout-type materials need to meet several high-level performance criteria, including high fluidity, low permeability, high early strength, corrosion protection, sulfate resistance, and, in some cases, frost durability.

One of the main aspects that cementitious grout manufacturers focus on when designing grouts is making them dimensionally stable. Ideally, non-shrink cementitious grouts would not exhibit dimensional changes in the plastic or hardened stages. Manufacturers try to eliminate the



inherent shrinking behavior of any cement-based material by adding expansive agents such as gas generation or ettringite.<sup>(6)</sup> However, comparatively little independent research has been done on this topic.

## **PREVIOUS RESEARCH ON GROUT PERFORMANCE**

Several research studies on the general mechanical performance of grout-type materials have been carried out in the last decades. (See references 6 and 14 through 16.) However, the field-cast grout-type materials specified for use in bridge connections have undergone limited research as to their relevance within this application. Graybeal conducted extensive research in which the performance of different grout-type materials intended to be used as bridge connections was evaluated.<sup>(17)</sup> One of the outcomes of that research was the wide range of grout performance that can be obtained, as well as the propensity of the materials to undergo volumetric deformations (e.g., expansion and/or contraction).

## **IC TECHNOLOGY**

IC has become more popular during the last years within the concrete community.<sup>(18-20)</sup> It is a technology that has shown multiple benefits in terms of concrete durability, especially in reducing shrinkage cracking. (See references 21 through 25.) While IC has been fortuitously included in concrete (particularly lightweight concrete) for many years, it is only within recent years that this technology has been intentionally incorporated into the system through the use of a variety of materials, including prewetted LWAs, superabsorbent polymers (SAPs), and prewetted wood fibers.

The concept supporting IC is the supply of highly porous particles in the concrete that can act as internal water reservoirs. These reservoirs will release the water from the inside of the concrete when negative pressure occurs in the cement matrix due to the formation of voids associated with chemical shrinkage. This process will provide a more homogeneous curing of the concrete, particularly for lower permeability (i.e., low water-to-cement ratio (w/c) concretes), which are more difficult to externally cure. A conceptual illustration of IC is provided in figure 2.

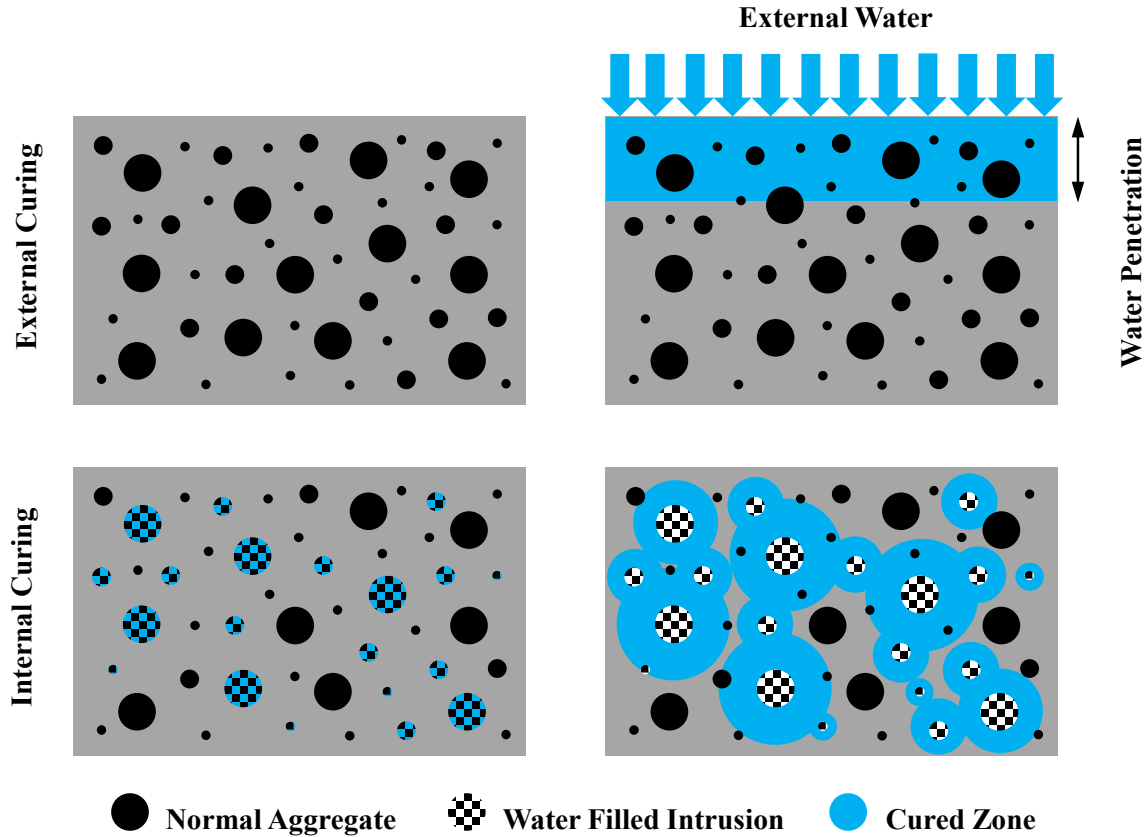


**Figure 2. Illustration. The differences between external curing and IC.**

The amount of IC water needed in a cementitious system is based on the chemical shrinkage occurring in the sample, as described by Bentz et al.<sup>(26)</sup> They formulated an equation that permits the calculation of the amount of LWA needed (see figure 3).

$$M_{LWA} = \frac{C_f \times CS \times \alpha_{max}}{S \times \phi_{LWA}}$$

**Figure 3. Equation. Amount of IC water needed based on the chemical shrinkage occurring in the sample.**

Where  $M_{LWA}$  lb/ft<sup>3</sup> (kg/m<sup>3</sup>) is the mass of LWA (in a dry state) that needs to be prewetted to provide water to fill in the voids created by chemical shrinkage,  $C_f$  lb/ft<sup>3</sup> (kg/m<sup>3</sup>) is the binder content of the mixture,  $CS$  (oz (mL) of water per lb (g) of binder) is the measured infinite chemical shrinkage of the binder as per ASTM C1608,  $\alpha_{max}$  (unitless) is the expected maximum degree of hydration,  $S$  (unitless) is the expected degree of saturation of the LWA and is typically taken as 1 when the dry LWA are water-soaked for 24 h (if absorption capacity is also measured at 24 h), and  $\phi_{LWA}$  (lb (kg) of water/lb (kg) of dry LWA) is the absorption capacity of the LWA (typically taken as the 24-h absorption measured value as per ASTM C1761).<sup>(27,28)</sup>

The implementation of this approach in grout-type materials has some difficulties, one being that the amount of reactive material in the solid fraction of a grout is typically unknown to the end-

user. This is important in order to estimate the binder content ( $C_f$ ), chemical shrinkage ( $CS$ ), and maximum expected degree of hydration ( $\alpha_{max}$ ) in figure 3. The approach followed in this study will be further discussed later in the report.



## CHAPTER 3. EXPERIMENTAL PROGRAM

### INTRODUCTION

A broad-scope research project on the performance of field-cast grout-type materials and their use in PBE connections is being conducted at the Federal Highway Administration (FHWA) Turner-Fairbank Highway Research Center. Graybeal et al. reported on an extensive grout-type materials characterization study.<sup>(17)</sup> One of the outcomes of that research was the wide range of grout performance that can be obtained as well as the propensity of the materials to undergo volumetric deformations. The purpose of the current report is to expand upon this work and present one of the focus points of the aforementioned research study: evaluation of dimensional stability of grout-type materials that may be used in PBE connections. This chapter describes the grout-type materials selected and testing procedures used for material and dimensional stability characterization. The approach followed in this research to provide IC in cement-based grouts is also discussed.

### MATERIALS AND MIXING PROCEDURES

A total of 11 grout-type materials of different nature and manufacturer were used in this study. Among them there were conventional grouts, repair materials, and a UHPC that could potentially be used as a grout in connections between prefabricated concrete elements. UHPC is a class of cementitious material designed to exhibit exceptional mechanical and durability properties.<sup>(29–31)</sup> All these materials provide two of the main properties required for grout-type materials: high flowability and high early-age strengths. The grout category, nomenclature used, and cost range are listed in table 1. Material categories were chosen based on past performance, applicability to onsite construction processes, and suitable published properties.<sup>1</sup> The grout is normally supplied in a bag containing the solid fraction (e.g., cementitious materials, additives, and fine aggregates) that is mixed with a certain amount of water following the recommendations of each of the grout's manufacturer, with the exception of the epoxy-based grouts, which are mixed with a resin and a hardener in the amounts also recommended by the manufacturer. The mixing details are summarized in table 2.

---

<sup>1</sup>These grouts are a representative sample of the types of grouts available on the open market. They cover much of the spectrum of available types of grouts. As such, other available grouts could have been selected for this study. FHWA does not endorse any product, service, or enterprise.

**Table 1. Grout-type materials used in the present study.**

<b>Grout Category</b>	<b>Nomenclature</b>	<b>Cost Range<sup>a</sup></b>
Non-metallic cement-based	G1	\$1,000 to \$2,000/yd <sup>3</sup>
Metallic cement-based	G2	\$1,000 to \$2,000/yd <sup>3</sup>
Non-metallic cement-based	G3	\$500 to \$1,000/yd <sup>3</sup>
Non-metallic cement-based	G4	\$1,000 to \$2,000/yd <sup>3</sup>
High-performance repair mortar	G5	\$1,000 to \$2,000/yd <sup>3</sup>
Epoxy-based	E1	\$4,000 to \$6,000/yd <sup>3</sup>
Epoxy-based	E2	\$4,000 to \$6,000/yd <sup>3</sup>
Fly ash-based rapid repair concrete	F1	\$1,000 to \$2,000/yd <sup>3</sup>
Magnesium-phosphate-based repair mortar	M1	\$1,000 to \$2,000/yd <sup>3</sup>
Magnesium-phosphate-based repair mortar	M2	\$4,000 to \$6,000/yd <sup>3</sup>
Ultra-high performance concrete	U3	\$2,000 to \$4,000/yd <sup>3</sup>

<sup>a</sup>Cost range estimated from cost purchasing values corresponding to the year 2013.

1 yd<sup>3</sup> = 0.765 m<sup>3</sup>

**Table 2. Mixing information of each of the grout-type materials.**

<b>Grout</b>	<b>Solid, lb (kg)</b>	<b>Water, lb (kg)</b>	<b>w/s</b>	<b>Solid Specific Gravity<sup>a</sup></b>	<b>Mix Time, min</b>	<b>Mixer Type</b>
G1	50 (22.7)	9.0 (4.1)	0.18	2.93	5	Concrete/mortar
G2	55 (25.0)	9.4 (4.3)	0.17	3.16	5	Concrete/mortar
G3	50 (22.7)	8.0 (3.6)	0.16	2.93	5	Concrete/mortar
G4	55 (25.0)	9.4 (4.3)	0.17	2.68	5	Concrete/mortar
G5	55 (25.0)	10.5 (4.8)	0.19	2.78	2	Concrete/mortar
E1	50 (22.7)	<sup>b</sup>	High flow	2.68	5	Concrete/mortar
E2	50 (22.7)	<sup>c</sup>	High flow	2.62	5	Concrete/mortar
F1	51 (23.2)	4.2 (1.9)	0.08	2.84	3	Bucket + paddle
M1	50 (22.7)	4.0 (1.8)	0.08	2.59	2	Concrete/mortar
M2	45 (20.4)	8.4 (3.8)	0.18	2.80	<sup>d</sup>	Bucket + paddle
U3	50 (22.7)	3.0 (1.6)	0.18 <sup>e</sup>	2.78	≈ 15	Concrete/mortar

<sup>a</sup>Specific gravity of the solids fraction measured using a gas (He) pycnometer.

<sup>b</sup>Resin component = 6 lb (2.7 kg); hardener component = 1.1 lb (0.5 kg).

<sup>c</sup>Resin component = 5.2 lb (2.4 kg); hardener component = 1.6 lb (0.7 kg).

<sup>d</sup>Mixing time based on time needed for the materials to achieve a temperature of 90 °F (32 °C). Time ranges from 10 to 15 min.

<sup>e</sup>Refers to water-to-binder ratio (w/b) as formulation is known.

The mixing amounts are based on the amount of solid that is contained in one bag (or bucket, when applicable). When evaluating grout-type materials, it is difficult to talk in terms of w/c or w/b because the reactive fraction of the solid is unknown. Instead, w/s is typically used. As observed, most of the grout-type materials had similar low w/s for high early-age strength development (0.16 to 0.19), with the exception of two of them (F1 and M1), which had an even lower w/s (0.08). U3 had a reported formulation, thus the value of 0.18 refers to the actual w/b. U3 also included the addition of chemical admixtures and steel fibers. The supplier of E1 and E2 recommends two formulations: standard and high flow. In this study, the high flow formulation was used. The specific gravity values of all the materials ranged from 2.59 to 3.16, inferring that the solid fraction is a mix of cementitious materials and fine aggregates. The high specific gravity value of the G2 grout was due to the presence of metallic particles in the solid fraction. Mixing times were typically 5 min (based on ASTM C1107), except for rapid set materials (G5, F1, M1), for which the mixing times were reduced according to the manufacturers' recommendations.<sup>(1)</sup> M2 and U3 had longer mixing times (about 10 to 15 min) also based on their manufacturers' recommendations. All grouts were prepared in either a mortar or concrete mixer (depending on batch size) except for F1 and M2, which were mixed in buckets with a drill and paddle (see figure 4). For more information about these materials, refer to appendix A.



**Figure 4. Photo. Mixing M2 grout using a drill and a paddle.**

## **FRESH PROPERTIES**

### **Initial Workability**

Since the materials selected in this study were intended to be used in the same type of application (i.e., as connections between prefabricated concrete elements), the comparative criterion chosen was to have similar fresh properties in terms of initial workability. This was done using the consistency definitions described in ASTM C1107, where the consistency is classified in three categories (plastic, flowable, and fluid) based on the flow measured in accordance with ASTM C1437.<sup>(1,32)</sup> In this study, plastic consistency was chosen, which corresponds to a flow increase between 100 and 125 percent of the original base diameter of the mold used in the flow test. (Although earlier in the report it was stated that grouts need to have high flowability, the plastic consistency described in ASTM C1107 is considered to be sufficient for placing and pumping purposes.) The flow of the grout was measured on the standard flow table after five drops in 3 s, as shown in figure 5. Then, the diameter was measured along the four lines marked on the table, and the average was recorded. This measurement was taken 7 and 15 min after mixing.



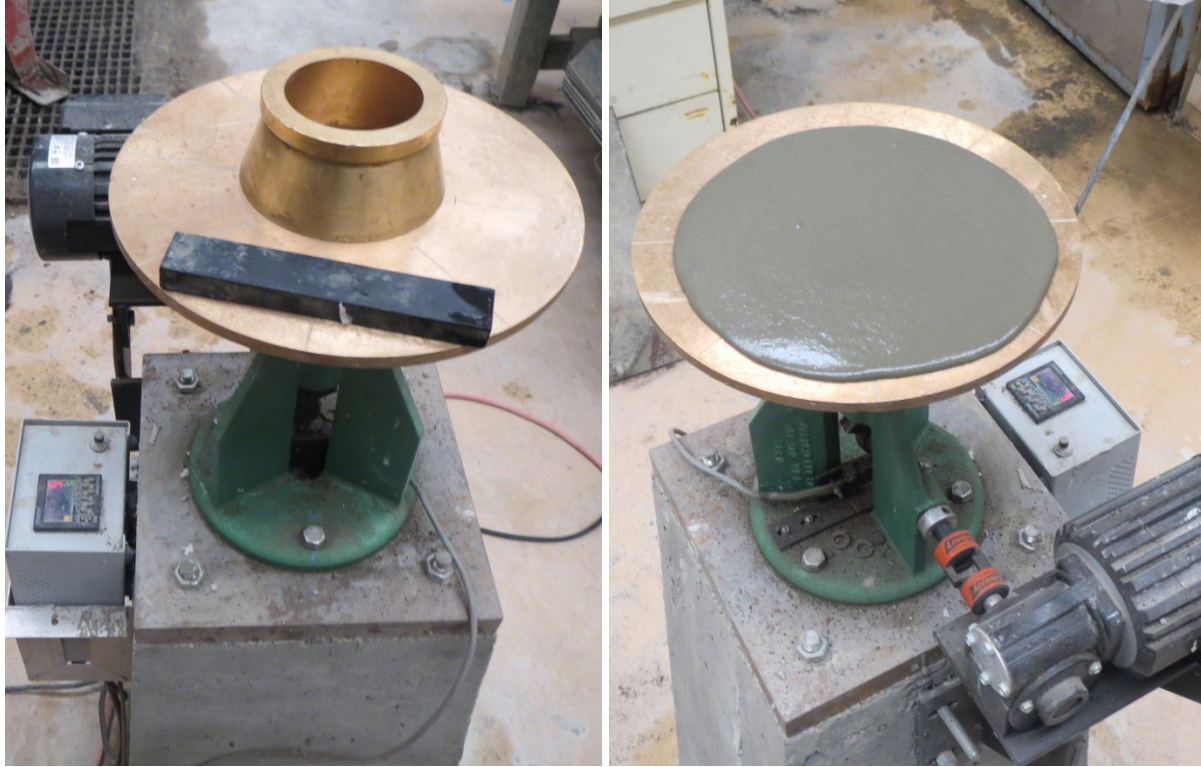


**Figure 5. Photo. Flow table test as per ASTM C1437, including accessories to run the test (left) and grout spread (right).<sup>(32)</sup>**

### **Air Content and Unit Weight**

The air content and unit weight of the mixtures were measured in the fresh state using the method described in ASTM C231 and ASTM C138, respectively.<sup>(33,34)</sup> The fresh material was poured in the measuring bowl of the air meter apparatus in one single layer (due to the high flowability of the material) and flushed with the top edge. In some cases (e.g., epoxy grouts), external vibration was needed to further consolidate the material in the bowl. Immediately after this process, the mass of the bowl and material was taken, and the previously measured mass of the bowl was subtracted. The result was divided by the known volume of the bowl, resulting in the unit weight of the material. Then, the air meter apparatus was assembled, and the air content was measured according to ASTM C231. The testing apparatus is shown in figure 6.



**Figure 6. Photo. Air content and unit weight.**

### **Set Time**

The set time of the mixtures was measured according to ASTM C403.<sup>(35)</sup> The test was based on measuring the pressure force needed to force a set of standard flat-headed needles to penetrate 1 inch (25.4 mm) into the material being tested, as shown in figure 7. The material was placed in a 6-inch (152-mm)-diameter by 6-inch (152-mm)-height cylinder and stored in a controlled environmental room at  $73.4 \pm 1.8$  °F ( $23 \pm 1$  °C) and a relative humidity (RH) of  $50 \pm 5$  percent. Readings were taken periodically after placing the material until a pressure of 4,000 psi (27.6 MPa) was reached, which indicates the time of final set, whereas a pressure of 500 psi (3.45 MPa) indicated the initial setting time. Two samples were used for this test. The data are plotted as pressure versus time after mix initiation. An example is shown in figure 8.

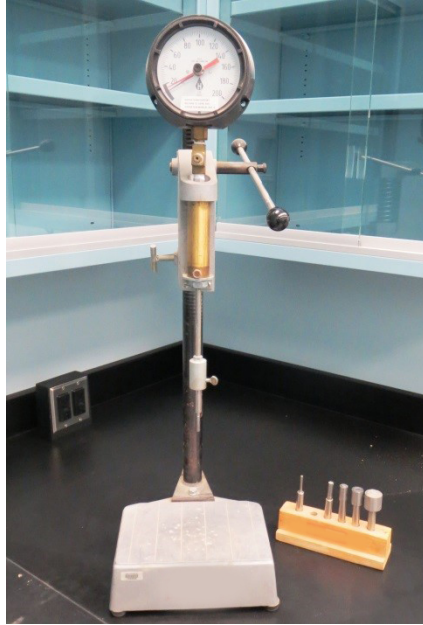
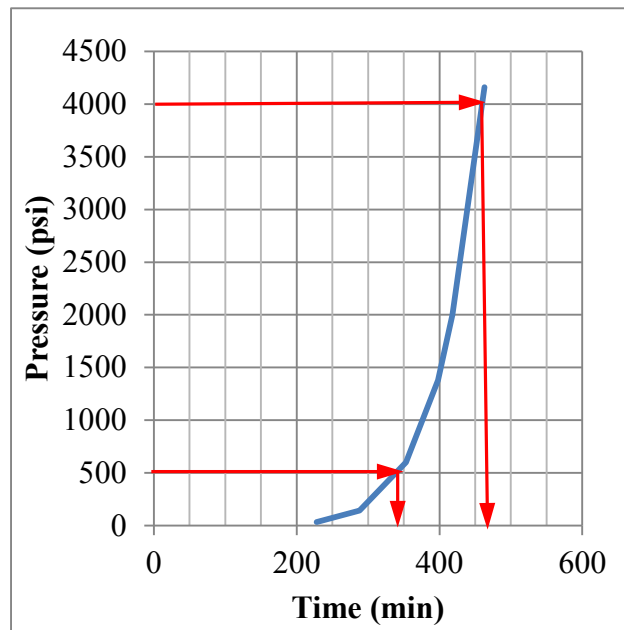


**Figure 7. Photo. Loading apparatus and penetration needles.**



1 psi = 0.007 MPa.

**Figure 8. Graph. Typical setting time data plot indicating initial and final set times.**

## HARDENED PROPERTIES

### Compressive Strength

For the evaluation of compressive strength, three 2-inch (51-mm) cube specimens (like those described in ASTM C109, see figure 9) were prepared according to ASTM C1107.<sup>(36,1)</sup> The cubes were tested at several ages: 4 and 8 h and 1, 3, 7, and 28 d. The cube specimens were kept

in their molds for 24 h, at which time they were demolded and sealed within plastic bags until the age of testing, unless the testing age was within the first 24 h, in which case, the specimens were tested immediately after being demolded.



**Figure 9. Photo. Compressive strength cube specimens (left) and cube specimen after test via ASTM C109 (right).<sup>(36)</sup>**

## **CHEMICAL PROPERTIES**

### **Heat of Hydration**

Numerous properties of cementitious materials are controlled by their initial hydration rate, volume change being one of them. One convenient way to measure the hydration reaction (rate and degree of hydration) is using isothermal calorimetry. An isothermal calorimeter was used in accordance with ASTM C1679, pictured in figure 10.<sup>(37)</sup> Approximately 0.25 oz (7 g) of an externally mixed material was weighed and placed in a glass ampoule, which was then capped and placed into the isothermal calorimeter about 10 min after mix initiation. The cumulative heat of hydration was measured during the first 7 d after mixing. It is important to mention that for some of the fast-setting grouts (typically the repair materials), it is difficult to detect the first heat release because it happens a few minutes after the solid-water contact.



**Figure 10. Photo. Isothermal calorimeter and sample specimens via ASTM C1679.<sup>(37)</sup>**

### **Chemical Shrinkage**

This test was performed in this study for IC design purposes. (Further details on IC mix design are provided later in the report.) The primary objective of any chemical shrinkage test is to quantify the change in volume that occurs as a result of hydration reactions. According to Le Chatelier, the volume of the hydration products in cementitious systems is lower than that of the initial reactants.<sup>(38)</sup> The chemical shrinkage is generally quantified by measuring the amount of water that is absorbed by a saturated sample, as described in ASTM C1608.<sup>(27)</sup> A thin layer of a fresh sample was placed in a glass vial, and the vial was filled with water. A rubber stopper with an inserted capillary tube was tightly placed in the vial. As the rubber stopper was inserted, the water level in the capillary tube rose. The test setup is shown in figure 11. This sample setup was placed on a horizontal surface in a controlled environmental room at  $73.4 \pm 1.8$  °F ( $23 \pm 1$  °C) and an RH of  $50 \pm 5$  percent. Three replicate samples were prepared. As hydration occurred, the water level in the capillary tube decreased. The volume decrease corresponds to the volume of chemical shrinkage and, thus, to the extent and rate of reaction. This is similar to the way that the extent and rate of reaction is captured using an isothermal calorimeter by measuring the heat release instead of the volume change.

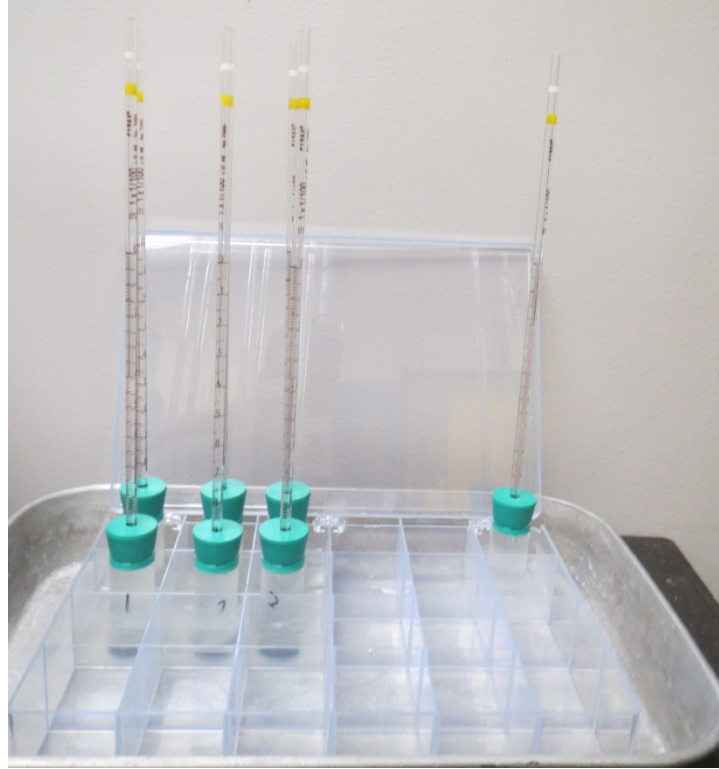


**Figure 11. Photo. Chemical shrinkage testing via ASTM C1608.<sup>(27)</sup>**

## **SHRINKAGE PERFORMANCE**

### **Shrinkage Performance Requirements According to ASTM C1107**

As previously mentioned, the ASTM C1107 standard specification covers packaged dry hydraulic cement non-shrink grouts.<sup>(1)</sup> One of the performance requirements stated in this specification is the allowed volume change that the grouts can undergo. Volume changes are measured in terms of height change of a cylindrical specimen through two other ASTM test methods, ASTM C827 *Standard Test Method for Change in Height at Early Ages of Cylindrical Specimens of Cementitious Mixtures* and ASTM C1090 *Standard Test Method for Measuring Changes in Height of Cylindrical Specimens of Hydraulic-Cement Grout*, for early-age (fresh) and hardened height changes, respectively.<sup>(39,40)</sup> The following sections describe these two test methods.

### ***ASTM C827***

The height change of a 3-inch (76-mm)-diameter by 6-inch (152-mm)-tall cylindrical specimen was measured in accordance with ASTM C827.<sup>(39)</sup> However, a modification of the ASTM C827 test method was made where a non-contact laser was placed above the specimen and used to measure the vertical distance from the laser to the indicator ball placed on the top surface of the specimen (see figure 12). This approach provided more simplicity in the execution of the test, rather than using a projector lamp, magnifying lens, and indicator charts as described in ASTM C827 (see figure 13). The laser approach has been compared with the original setup, and similar results were obtained.<sup>(41)</sup> The measured vertical distance corresponds to the increase or decrease

in height (expansion or shrinkage) of the material laterally confined in the cylindrical mold from the time of molding to when the mixture becomes hard (i.e., final set).

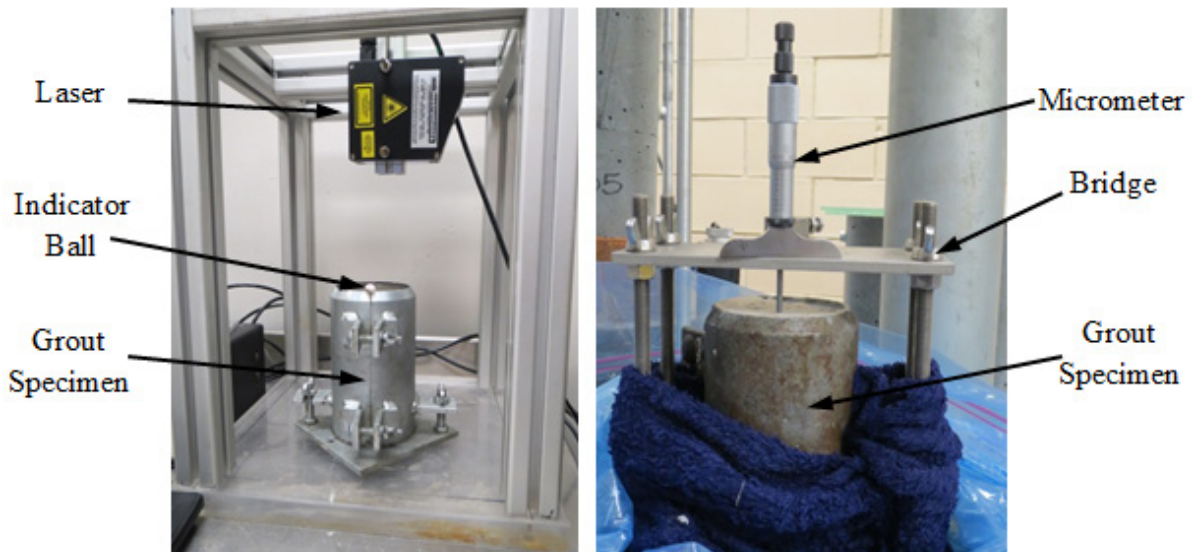


**Figure 12. Photo. Modified ASTM C827 setup (left) and change length in a hardened specimen with ASTM C1090 (right).<sup>(39,40)</sup>**

### ***ASTM C1090***

Two cylindrical specimens with the same dimensions as those used for the ASTM C827 test method were prepared in which the change in height was measured at four points on the top surface of the specimens using a micrometer in accordance with ASTM C1090 at 1, 3, 7, 14, and 28 d (see figure 12).<sup>(40)</sup> An initial four-reading measurement was taken right after placing a glass plate on top of the fresh sample surface. The glass plate was removed from the top of the test specimen after 24 h. After removal, the thickness of the glass plate was measured with a caliper at the points of contact between the glass plate and the micrometer. This thickness was then added to the four-reading initial measurement.

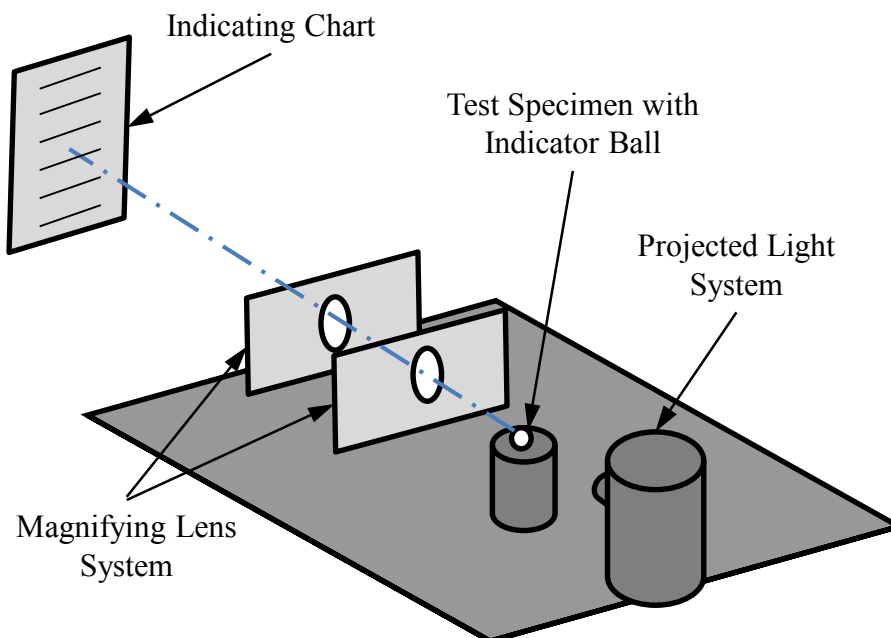


**Figure 13. Illustration. The apparatus for early change in height adapted from ASTM C827.<sup>(39)</sup>**

In both test methods, there is always a certain degree of friction between the specimen's sides and the inner surface of the metallic mold. The degree of restraint varies with the mixture viscosity and degree of hardening. Though not recommended by the ASTM standards, and in order to provide the lowest friction possible, an acetate sheet was used in between the test specimen and the mold. The height change results in both test methods are expressed in terms of percentage increase or decrease of the original specimen height.

### **Autogenous and Drying Deformations**

Autogenous deformation was assessed using an automated version of the sealed corrugated tubes test, as described in ASTM C1698.<sup>(3)</sup> Three replicate specimens were evaluated concurrently. The tubes were placed over supports provided with spring-loaded linear variable differential transformers at each end that were connected to a data acquisition system. The displacement (converted to strain) was measured every 5 min for 7 d (see figure 14). The autogenous deformations were zeroed at the final time of set measured as described in ASTM C403.<sup>(35)</sup> To guarantee isothermal conditions, the specimens were kept in an environmental room at  $73.4 \pm 1.8$  °F ( $23 \text{ °C} \pm 1 \text{ °C}$ ) and an RH of 50 percent  $\pm 5$  percent. The mass of the samples was taken at the beginning and after 7 d of testing to confirm that the specimens were properly sealed. For later age measurements, four 1 by 1 by 12 inch (25 by 25 by 305 mm) prismatic specimens were prepared in accordance with ASTM C157, in which all four faces were sealed with two layers of aluminum tape after removal from the molds at 24 h.<sup>(2)</sup> Similar samples were prepared without aluminum tape for shrinkage assessment in drying conditions (see figure 14). The specimens were kept in the same environmental room as the corrugated tubes. Length change measurements, as well as mass measurements, were taken every week for the first month and once a month for the next 6 mo.





**Figure 14. Photo. ASTM C1698 tubes setup (top) and sealed and drying ASTM C157 specimens (bottom).**<sup>(3,2)</sup>

## IC APPROACH

### Introduction

Given the fact that cement-based grouts commonly exhibit shrinkage, this research also included additional tests focused on IC, which has become more popular during the last several years within the concrete community.<sup>(18–20)</sup> As previously mentioned, there are several materials available for providing IC, including prewetted LWAs, SAPs, and prewetted wood fibers. In this study, prewetted LWAs were used.

Non-shrink cementitious grouts are often pre-packaged and can be extended using small aggregate for volumetrically large pours. IC can be thought of as an extension of the grouts using LWA rather than normal weight aggregate. The primary reason for using IC is to reduce shrinkage, especially during the first days when the tensile strength of the material is still low. In

addition, this technology might be helpful in improving curing conditions in some locations where conventional (i.e., external) curing is difficult or impossible to implement, as well as in providing some robustness to the surface preparation (in terms of moisture content) of the precast (or existing) concrete elements since prewetted LWA also may serve as additional reservoirs if water is drawn from the grout into the substrate.

### **Mixture Proportioning with IC**

The fine LWA used in this study consisted of rotary kiln expanded shale with a specific (dry) gravity of 1.56 and a 24-h water absorption of 16.95 percent by dry mass. The initial idea was to use the equation that Bentz et al. formulated based on the chemical shrinkage occurring in the sample (see figure 3).<sup>(26)</sup> However, as previously mentioned,  $C_f$ ,  $CS$ , and  $\alpha_{max}$  (as shown in figure 3) cannot be estimated unless the reactive content of the solid is known. Petrography was used to facilitate estimation of the reactive content. This technique uses a polarized light microscope to differentiate between crystalline and amorphous materials. In addition, cementitious materials have sufficient differences in their raw feeds, burning temperatures, mineral phases, and microstructure that it is possible to differentiate them, thus identifying particles such as cement, fly ash, and slag.

Two of the cementitious grouts were engaged within the IC portion of the study, namely G2 and G4. The petrographic analysis demonstrated that the cementitious contents were approximately 35 and 30 percent by mass, respectively. With this information and the known water contents, the theoretical w/b for each of the grouts could be calculated, resulting in w/b equaling 0.56 and 0.49 for G2 and G4, respectively. Consequently,  $\alpha_{max}$  in figure 3 could be considered to be 1 because the w/b in both cases was above 0.42.<sup>(42)</sup>

Likewise, chemical shrinkage of the two grouts was measured according to ASTM C1608, and the results were normalized by the amount of reactive material of each of the grouts.<sup>(27)</sup> The infinite chemical shrinkage could be then evaluated by plotting the chemical shrinkage over the inverse of the time, resulting in values of 1.99 and 2.15 fl oz/lb (0.13 and 0.14 mL water/g) binder for G2 and G4, respectively. (See chapter 4 of this report.) These values are high compared with plain cement (0.98 fl oz/lb (0.064 mL water/g)), which is an indication of the presence of other cementitious materials that typically have higher values of chemical shrinkage.<sup>(38)</sup> Note that while petrographic images showed fly ash and slag particles, scanning electron microscope (SEM) images confirmed the presence of silica fume in both grouts. Figure 15 provides petrographic and SEM images that show fly ash, slag, and silica fume particles.

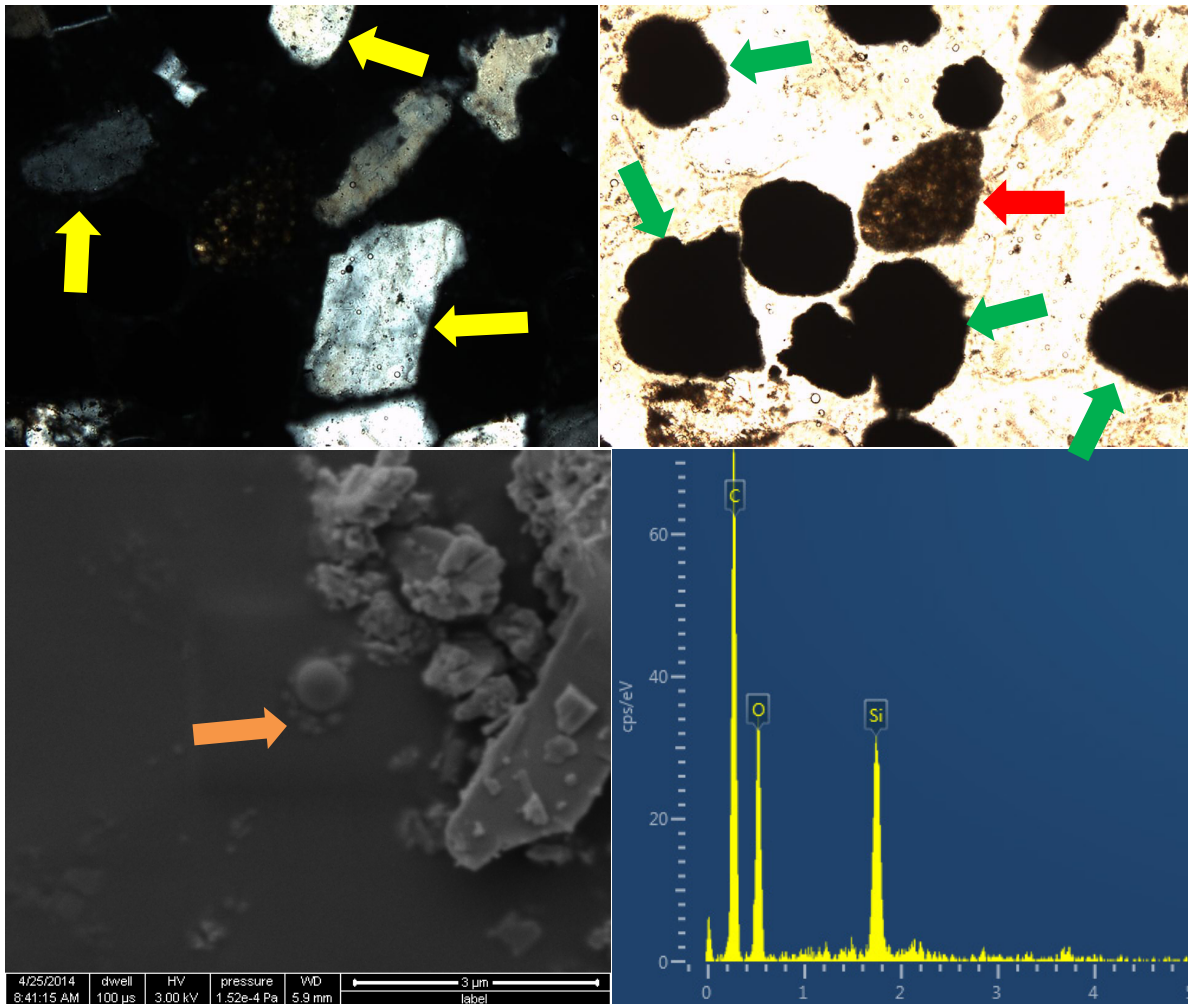


**Figure 15. Photo. Images taken in G4 dry samples: cross-polarized light thin section micrograph with yellow arrows showing non-reactive sand particles (top left); plane-polarized light of the same thin section micrograph with red and green arrows showing cement and fly-ash particles, respectively (top right); SEM image with orange arrow showing a silica fume particle (bottom left); and energy-dispersive X-ray spectroscopic analysis confirming the siliceous nature of the silica fume particle (bottom right).**

An appropriate IC design is crucial from the viewpoint of durability. In an overdosed system, if some LWAs remain filled with water, it may have detrimental effects from a freeze/thaw perspective. In this study, prewetted LWA were added to the base grout formulation at a mass calculated using figure 3 for each of the grouts. It is recognized that this addition of LWA will change the paste content of the formulation with respect to the total volume, thus having an influence on the shrinkage performance. However, it is determined to be a reasonable path given the lack of knowledge of the proprietary grout constituents. Table 3 shows the mixture proportions of G2 and G4 including IC.

**Table 3. Mixture proportions of the internally cured cement-based grouts.**

<b>Component</b>	<b>Mixture Proportions, kg</b>	
	<b>G2 - 0.17 - IC</b>	<b>G4 - 0.17 - IC</b>
Solid	25.0	24.9
LWA	5.8	7.2
Mixing water <sup>a</sup>	5.2	5.5

Note: Mass of the solids corresponds to the mass of one bag.

<sup>a</sup>Total water including w/s mixing water and water that is absorbed by LWA.

1 lb = 0.45 kg.

## CHAPTER 4. RESULTS AND DISCUSSION

### INTRODUCTION

This chapter presents all the results obtained during the execution of the research project. The results are presented in three sections: (1) workability and strength, (2) dimensional stability, and (3) IC. The first section shows that all the grout-type materials selected for this study had similar initial flow along with sufficient early strength, as required for grout-type materials. (As previously mentioned, the grouts were intended to be used in the same type of application: connections between prefabricated concrete elements. Thus, the comparative criterion chosen was to have similar initial workability.) The second section is the main focus of this research and includes results on dimensional stability. While some of these results were collected using tests required by the specification for grouts (i.e., ASTM C1107), other results were obtained from additional standardized tests in order to more fully characterize dimensional stability.<sup>(1)</sup> The appropriateness of using these different tests is also discussed in this section. Finally, the third section presents the strength and dimensional stability results obtained for the internally cured cement-based grouts.

Note that all test methods used in this study are intended for use with cementitious materials. Therefore, some of the materials are not necessarily suitable for these test methods. This limitation will be further discussed in this chapter. Also, note that the exact formulation or composition of grout-type materials is typically unknown to the end-user because they are proprietary materials. As such, it can be challenging to develop causal relationships between the materials and their performance in terms of workability, reactivity, strength, and volume change.

### WORKABILITY AND COMPRESSIVE STRENGTH

The initial grouts' consistency (or workability), final set time, air content, and unit weight are summarized in table 4. The flow measurements were taken 7 and 15 min after the solid-water first contact except for G5 and M1, in which cases the flow was taken at 3 and 7 min due to final setting time limitations, and U3, which was only measured at 15 min. In all cases, except for the G5 grout, the material consistency at 7 min was within the plastic consistency range described in ASTM C1107, which is between 100 and 125 percent of the original base diameter of the mold used in the flow table test.<sup>(1)</sup> The flow of the epoxy grouts could not be measured due to the "sticky" nature of the material, which made it difficult to lift the mold without disturbing the material. The fact that all grouts had similar initial consistency is indicative of the possibility of using these materials in the same type of application (i.e., connections between prefabricated concrete elements). However, the consistency was not within the above mentioned range for some of the grouts at 15 min. The degree of workability loss is normally related to the type of chemical admixtures used in the material. Since the formulation in most of the materials is unknown, it is difficult to make conclusions in this regard. The 7-min flow for the U3 material could not be measured due to mixing time requirements; in any case, it exceeded the upper threshold of 125 percent at 15 min.

**Table 4. Flow measurements using ASTM C1437 methods, set time, fresh air content, and unit weight.<sup>(32)</sup>**

<b>Grout</b>	<b>Number of Drops</b>	<b>Flow at 7 min, Percent<sup>a</sup></b>	<b>Flow at 15 min, Percent</b>	<b>Final Time of Set, h<sup>(35)</sup></b>	<b>Air Content, Percent<sup>(33)</sup></b>	<b>Unit Weight, lb/ft<sup>3(34)</sup></b>
G1 - 0.18	5	117	84	6.8	5.1	0.129
G2 - 0.17	5	110	91	6.8	3.6	0.153
G3 - 0.16	5	112	106	7.7	3.4	0.139
G4 - 0.17	5	111	100	10.3	12.0	0.122
G5 - 0.19 <sup>b</sup>	5	80	70	0.3	3.1	0.134
E1 - high flow	c	c	c	1.4	4.4	0.135
E2 - high flow	c	c	c	3.5	8.5	0.130
F1 - 0.08	5	101	109	0.7	4.6	0.146
M1 - 0.08 <sup>b</sup>	5	115	75	0.4	6.9	0.135
M2 - 0.18	5	> 125	<sup>d</sup>	0.3	<sup>d</sup>	<sup>d</sup>
U3 - 0.18	5	<sup>e</sup>	>125	6.9	3.2	0.160

1 lb/ft<sup>3</sup> = 16.02 kg/m<sup>3</sup>

<sup>a</sup>Flow slightly changes depending on mixer used.

<sup>b</sup>Flow was measured at 3 and 7 min due to final setting time limitations.

<sup>c</sup>Material sticks in mold. Test cannot be performed.

<sup>d</sup>Not measured due to final setting time limitations.

<sup>e</sup>Flow was measured only at 15 min due to mixing time requirements.

It is interesting to note how the workability of the F1 grout increased from 7 to 15 min when considering the fast-setting behavior that developed. (Final set was achieved at 45 min.) Although not reported by flow values, E2 was slightly more flowable than E1. Both grouts also showed short setting times, similar to G5, F1, M1, and M2 (less than 4 h). All of these grouts were designed to be fast-setting repair materials. The kinetics of the chemical reactions of these (repair) materials may have been different from that of the cement-based grouts. For instance, G5 may have been a calcium sulfoaluminate cement-based grout, F1 appeared to be a high-calcium fly-ash-based material, M1 and M2 were polymer-modified cementitious material (i.e., magnesium phosphate), and E1 and E2 were epoxy-resinous materials. The other grouts showed final set times in the range of 6 to 10 h, as typically observed in fast-setting cement-based materials. Air content ranged from low values (3.1 percent) up to high values (12.0 percent). Unit weight values correlated to the measured air content in that high air content corresponded to low unit weight.

The strength obtained for the grouts included in this research study are presented in table 5. In addition, the compressive strength required by ASTM C1107 is shown in table 6.<sup>(1)</sup> Despite the fact that the other materials used in this research are not grouts per se (they are either repair materials or UHPC), they were tested according to the abovementioned ASTM specification due to their similar performance. As shown in table 5, all the grouts complied with the minimum strength requirements at all ages, except for the M2 grout that did not achieve the strength required at 28 d. Particular attention is given to U3, depicting strength values that considerably exceeded the minimum requirements. This is normal because this type of material is designed to exhibit exceptional mechanical and durability properties. While G5, E1, E2, F1, M1, and M2 developed strength within the first 8 h (which is consistent with the rapid setting times

previously reported), a slower strength development was observed in the other cement-based grouts (G1 through G4), but still it was enough to exceed the minimum strength required at each age.

**Table 5. Compressive strength results for grout cubes.**

Grout	Average Compressive Strength, psi					
	4 h	8 h	1 d	3 d	7 d	28 d
G1 - 0.18	a	a	3,713 (62) <sup>b</sup>	5961 (128)	6,541 (141)	7,281 (335)
G2 - 0.17	a	a	5,018 (109)	7,150 (222)	8,833 (15)	9,805 (219)
G3 - 0.16	a	a	4,424 (120)	7,092 (321)	7,600 (170)	9,805 (290)
G4 - 0.17	a	a	2,408 (75)	3,800 (110)	5,149 (25)	6,338 (60)
G5 - 0.19	6,991 (238)	7,556 (255)	8,224 (409)	10,153 (205)	11,008 (203)	10,428 (94)
E1 - high flow	696 (71)	5,424 (215)	10,283 (67)	10,051 (157)	11,095 (231)	11,168 (486)
E2 - high flow	a	1,224 (20)	8,137 (210)	10,660 (46)	11,197 (55)	13,547 (474)
F1 - 0.08	4,496 (30)	5,018 (197)	5,062 (152)	6,382 (128)	8,006 (149)	8,137 (55)
M1 - 0.08	4,641 (297)	4,525 (59)	6,237 (307)	6,512 (277)	6,411 (180)	7,817 (341)
M2 - 0.18	3,960 (86)	4,322 (126)	4,670 (197)	4,946 (97)	4,485 (43)	4,767 (207)
U3 - 0.18	93 (17)	734 (23)	13,510 (41)	18,811 (500)	19,159 (231)	24,714 (131)

1 psi = 0.007 MPa

<sup>a</sup>Material had not set yet or it was still too weak to be tested.

<sup>b</sup>Numbers in parentheses indicate one standard deviation in psi as determined for three replicate specimens tested at each age.

**Table 6. Minimum compressive strength for 2-inch (51-mm) cubes according to ASTM C1107.<sup>(1)</sup>**

Testing Age (d)	Compressive Strength, psi
1	1,000
3	2,500
7	3,500
28	5,000

1 psi = 0.007 MPa

## Discussion of the Results

A detailed material characterization is needed to better understand the workability and strength development results. As previously mentioned, the degree of workability loss is normally related to the type of chemical admixtures used in the material. On the other hand, strength gain, at least for the cement-based grouts and the UHPC (G1, G2, G3, G4, and U3), directly depends on the raw material composition, reactivity, fineness, capillary porosity (i.e., initial water content), and the degree of hydration achieved (0 to 1). The degree of hydration was expected to be close to 1, at least for the cement-based grouts, since the w/b is likely high when considering the binder content of each grout (as already explained in the Mixture Proportioning with IC section in chapter 3). G5 was also a cement-based grout; however, a fast-set cement type (e.g., calcium sulfoaluminate) is suspected to have been included due to the high strength development after a few hours of hydration. Therefore, the strength development in G5 is mainly driven by the

reactivity of the material. Similar reasons might be given to explain the early strength achieved in the other type of materials (E1, E2, F1, M1, and M2). The kinetics of the chemical reactions in these materials is different from that of cement-based grouts. E1 and E2 are two-component, epoxy-based materials in which a chemical reaction occurs when the resin (component A) is mixed with the hardener (component B) to form polymers; thus, the reactivity depends on the type of polymerization. M1 and M2 are magnesium phosphate-based materials where magnesia and phosphate react with water to form magnesium phosphate to provide strength. Finally, F1 appears to be a high-calcium fly-ash-based material with some kind of polymerization (i.e., activation), which also depends on the type of polymers that form in the system.

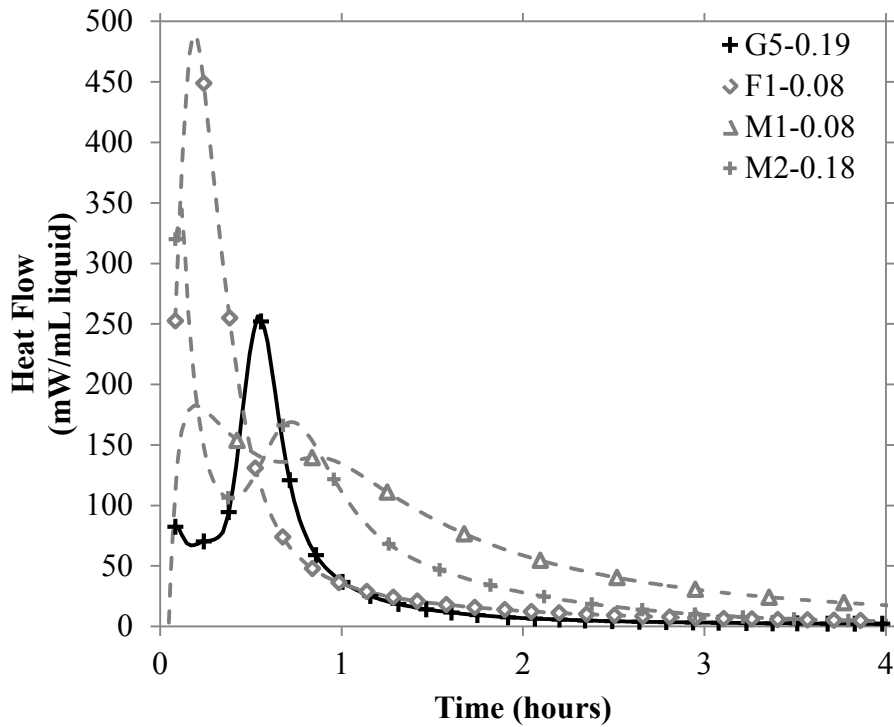
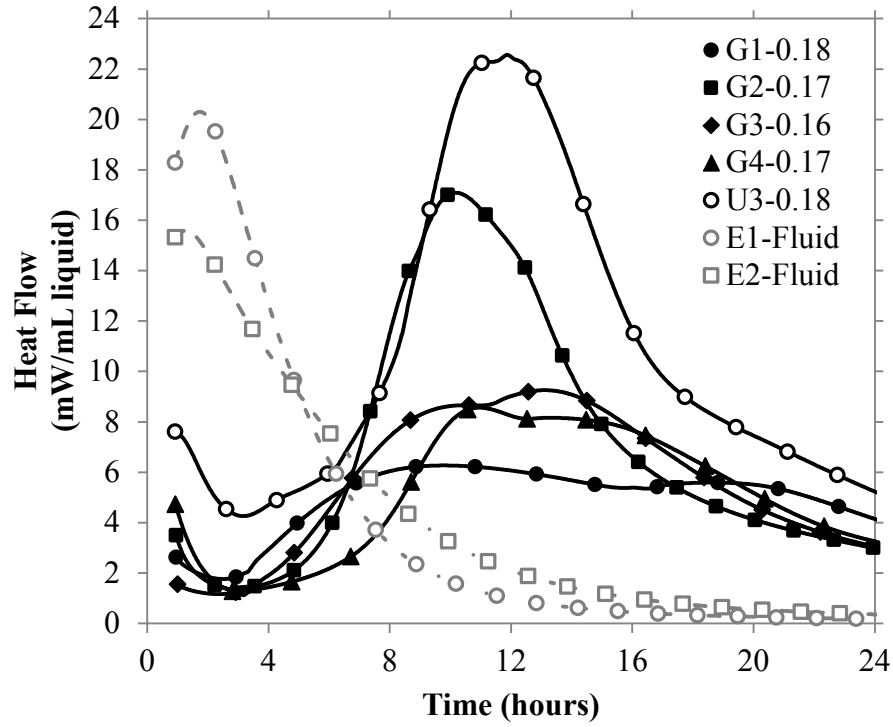
## **DIMENSIONAL STABILITY**

### **Grouts Reactivity**

Typically, chemical reactions occurring in grout-type construction materials result in volume changes of the materials. This means that the evaluation of the extent and rate of reaction would be indicative of the amount of volume change occurring in the system. Since most of these reactions are exothermic, this can be done by measuring the heat that is released when the solids react with the mixing water. However, heat being released is only indicative of the reaction occurring in the system. In order to evaluate whether this reaction implies expansion or contraction of the material, it would be necessary to use other (chemical) tests. This was not done in this research. Thus, the reactivity results included in this report only provide important contextual information of the timing of key reactions taking place.

The heat release was measured using an isothermal calorimeter. The results are shown in figure 16 (note different scale in the X-Y axis of both plots). The results were normalized by the initial porosity of the mixes (i.e., ounces (milliliters) of mixing water), which is common practice when comparing different materials with different water contents, as in this case. As observed in figure 16, the cementitious grouts G1, G2, G3, and G4 as well as the U3 depicted calorimetry curves typical from cementitious materials (i.e., with two differentiable peaks, one that is indicative of silicates reaction, and the other one that is indicative of aluminates reaction). The main (first) peak times in these materials ranged from 8 to 12 h. M1 and M2 also showed two differentiable peaks, but they occurred much faster than in the cementitious grouts (within the first hour). In addition, the magnitude of these peaks was much larger than that of the cementitious grouts. The fast reaction seemed to be common in magnesium phosphate-based materials, typically used as repair materials. Both E1 and E2 only showed one main peak at about 2 h after mixing. Similarly, the other two repair materials (F1 and M2) only showed one main peak, but this occurred faster and in a larger magnitude compared with that of E1 and E2. The appropriateness of using isothermal calorimetry to measure the heat release in repair materials is questionable due to the very fast reaction as well as the very large heat values observed. A different approach to measure the reactivity of some of the repair materials may be more appropriate.





1 oz = 29.6 mL

**Figure 16. Graph. Heat flow during the first hours of reaction: no repair materials (low heat) (top) and repair materials (high heat) (bottom).**

## Dimensional Stability According to ASTM C1107

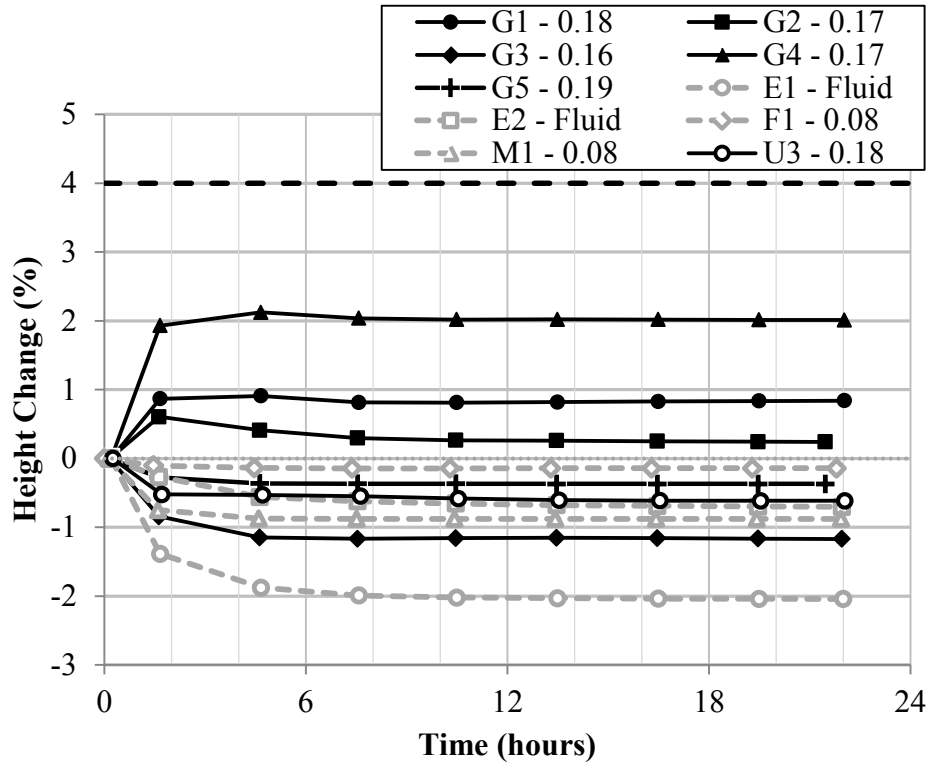
ASTM C1107 evaluates the dimensional stability of grouts in terms of the change in height of cylindrical specimens.<sup>(1)</sup> The specification establishes maximum and minimum height change values that can be measured using two ASTM standard specifications: (1) ASTM C827 for fresh-stage height changes and (2) ASTM C1090 for hardened-stage height changes.<sup>(39,40)</sup> The height change requirements are shown in table 7.

**Table 7. Height change requirements according to ASTM C1107.<sup>(1)</sup>**

<b>Early Age Height Change Maximum Percent at Final Set (ASTM C827)<sup>(39)</sup></b>	<b>Hardened Height Change Maximum and Minimum Percent at 1, 3, 14, and 28 d (ASTM C1090)<sup>(40)</sup></b>
+ 4.0	+ 0.3 0.0

### *ASTM C827*

The height change results obtained at early ages (i.e., fresh stage) are presented in figure 17. The measurements were collected following a modified version of the ASTM C827 specification (figure 12 (left)).<sup>(39)</sup> The results show that none of the mixtures exceeded the 4 percent maximum expansion allowed by ASTM C827 (indicated by a dashed line). However, some of the grouts exhibited a height reduction. These include two of the cement-based grouts (G3, G5), the UHPC (U3), and the non-cement-based grouts (F1, E1, E2, and M1). M2 could not be tested due to setting time limitations. The reduction in height was less than 1 percent for all cases, except for G3 and E1, which exceeded this value. ASTM C1107 does not specify any height reduction limitation during the fresh stage (table 7).<sup>(1)</sup> However, if it is assumed that the specification does not allow any reduction in height, then these grouts exhibiting height reduction would not comply with the standard. On the other hand, if ASTM C1107 is read to only limit the height increase, then all of the grouts comply with the standard. In all cases, a relatively rapid increase or decrease in height is observed from the beginning of the test until each of the grouts reaches final set (see table 4 for setting times), after which the curves transition to a plateau.



Note: Only one specimen was tested for each grout.

**Figure 17. Graph. Change in height at early ages according to a modified version of ASTM C827.<sup>(39)</sup>**

This test provides information about volume changes occurring between the time immediately after mixing and that of final set. The volume changes measured include: expansion (e.g., expansive agents and thermal), chemical and autogenous shrinkage (which before set have similar values), surface settlement, plastic shrinkage due to drying of the specimen from the top surface, and some error given by the settlement of the ball on the top surface.<sup>(44)</sup> Due to the presence of all these parameters, the measurements are primarily useful for comparative purposes.

### ***ASTM C1090***

Table 8 shows the height change results obtained during the hardened stage, according to ASTM C1090.<sup>(40)</sup> In a general sense, it is not possible to quantitatively compare the results obtained during the first 24 h with those in figure 17 (fresh stage) since the curing conditions are different. In the C1090 case, the specimens were sealed in a plastic bag throughout the test duration; therefore, the parameters that can be considered in this test are chemical and autogenous shrinkage and surface settlement. In other words, the change in height does not include the effects of drying. As with the early height change test, the results are merely comparative.

**Table 8. Height change of hardened grouts via ASTM C1090 test.<sup>(40)</sup>**

Grout	Average Height Change of Hardened Grout at a Given Age (Percent) <sup>a</sup>				
	1 d	3 d	7 d	14 d	28 d
G1 - 0.18	0.0	0.0	0.0	0.0	0.0
G2 - 0.17	0.0	0.0	0.0	0.0	0.0
G3 - 0.16	-1.2	-1.2	-1.2	-1.2	-1.2
G4 - 0.17	0.0	0.0	0.0	0.0	-0.1
G5 - 0.19	-0.7	-0.7	-0.7	-0.7	-0.7
E1 - high flow	-0.2	-0.2	-0.2	-0.2	-0.2
E2 - high flow	-0.2	-0.2	-0.2	-0.2	-0.2
F1 - 0.08	-0.2	-0.2	-0.2	-0.2	-0.2
M1 - 0.08	-0.1	-0.1	-0.1	-0.1	-0.1
M2 - 0.18	b	b	b	b	b
U3 - 0.18	-0.4	-0.4	-0.4	-0.4	-0.4

<sup>a</sup>Maximum and minimum expansion allowed by ASTM C1090 is 0.3 and 0.0 percent, respectively.<sup>(40)</sup>

<sup>b</sup>M2 could not be tested due to setting time limitations.

The results show that three of the cement-based grouts (G1, G2, and G4) did not exhibit any contraction or expansion throughout the test duration. It is interesting to note that these are the same grouts that exhibited expansion in the ASTM C827 test (see figure 17).<sup>(39)</sup> One aspect to point out about the ASTM C1090 test procedure is that the glass plate used to cover the top surface of the specimen during the first 24 h prevented the specimen from expanding.<sup>(40)</sup> The glass plate was held down with a plunger that was attached to a bridge. This is the reason why none of the grouts expanded within the first day, when expansive agents (if present) would act to counteract the possible shrinkage. The rest of the grouts showed a decrease in the specimen height, with the greatest decrease exhibited by G3. These are the same grouts that showed a height reduction in figure 17. M2 could not be tested due to setting time limitations. As already mentioned, the curing conditions of ASTM C827 and ASTM C1090 test methods are different (sealed versus drying); however, the same trends were observed in regards to the height increase or reduction.<sup>(39,40)</sup> Therefore, due to the fact that ASTM C1090 does not permit any height reduction, all grouts exhibiting a cumulative height reduction (i.e., G3, G5, E1, E2, F1, M1, M2, and U3) are considered to have not met the requirements of ASTM C1107.<sup>(1)</sup>

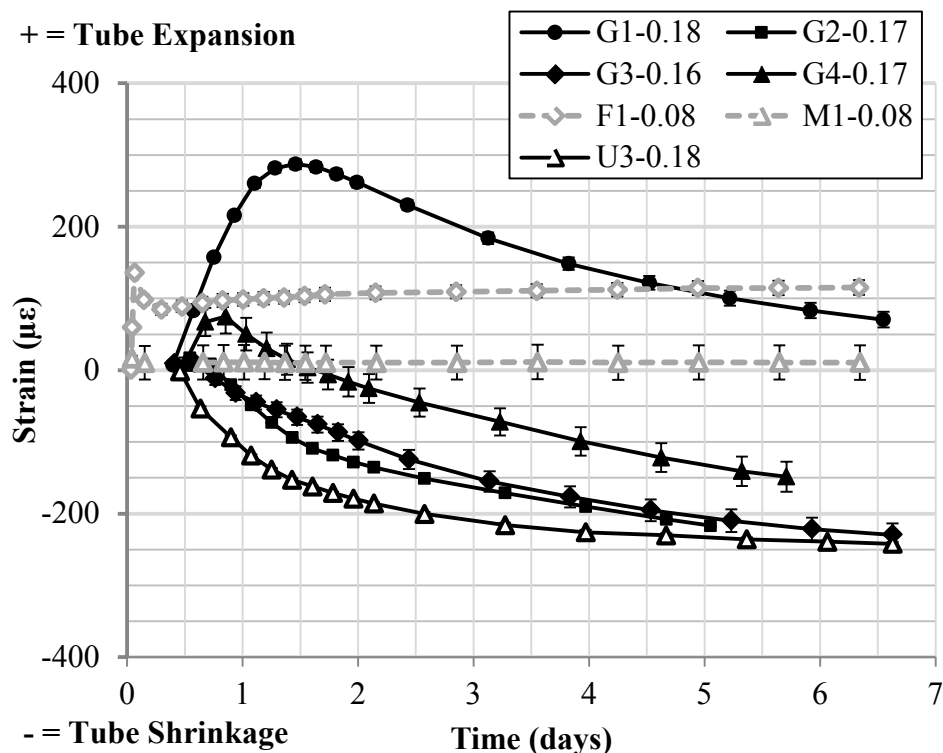
### Autogenous and Drying Deformations

As mentioned before, many of the grouts tested do not appear to comply with ASTM C1107 in terms of height reduction.<sup>(1)</sup> On the other hand, some of the cementitious grouts, including G1, G2, and G4, show either expansion or an absence of both expansion and contraction (depending on the test method used). Hence, a user might infer from the test method that these three materials do not shrink. This is very important because shrinkage may result in shrinkage cracking (causing the degradation of the material) and could, in the type of application studied in this research, also imply loss of bond to the concrete substrate. This section is focused on pure shrinkage deformations in both sealed (i.e., autogenous) and drying conditions, these being cases not considered by the ASTM C1107 standard.<sup>(1)</sup> These curing conditions are important from the

viewpoint of the materials' application because some of the precast connections will be largely enclosed (sealed), while others will be partially exposed to the environment (drying).

### ASTM C1698

The autogenous shrinkage results measured in accordance with ASTM C1698 are presented in figure 18.<sup>(3)</sup> The results are expressed as a function of time, from the time of final set to 7 d of reaction. Some of the grouts solely exhibited shrinkage (G2, G3, and U3), others showed an initial expansion followed by shrinkage (G1 and G4), and others exhibited a fairly constant expansion at all times (F1 and M1). While E1 and E2 could not be tested due to the difficulty of properly consolidating the material in the corrugated tubes, G5 and M2 were not tested due to setting time limitations. As mentioned before, this test is designed for cementitious materials, typically more fluid and with longer setting times than these non-cementitious and repair materials type. Finally, U3 was prepared without steel fibers due to the difficulty encountered when attempting to insert the fiber reinforced material into the corrugated tubes. If fibers were added, less shrinkage deformation would be expected due to the internal restraint provided by the fibers.



Note: Error bars indicate one standard deviation as determined for three replicate specimens.

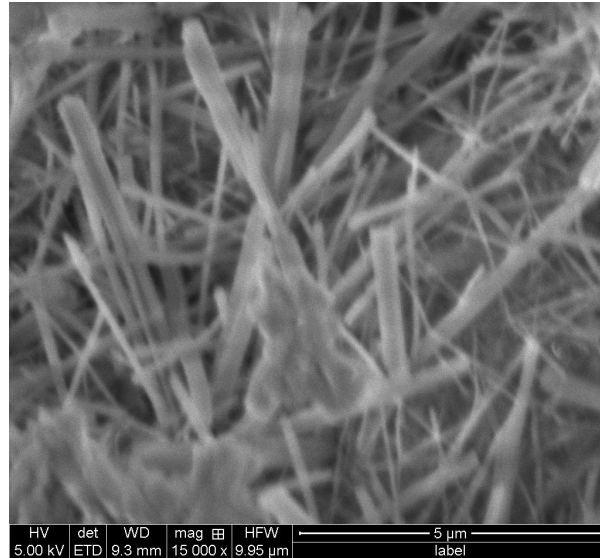
**Figure 18. Graph. Autogenous (sealed) shrinkage as a function of time via ASTM C1698.<sup>(3)</sup>**

### Discussion of Results

As seen in figure 18, all of the cement-based grouts used in the study, including UHPC, show autogenous shrinkage at some point, which is common in cement-based materials. It is worth mentioning that the cement-based G1 grout also shrinks, despite showing a net positive

deformation of about  $70 \mu\epsilon$  after 7 d. When evaluating the risk of shrinkage cracking, the net difference between the maximum and minimum deformations achieved during the test should be considered.<sup>(45)</sup> Typically in cement-based grouts, low w/s decreases particle spacing (and pore sizes), contributing to an increase of the autogenous shrinkage. However, “non-shrink” grout-type materials are usually designed to undergo autogenous expansion during the first hours of the hydration reaction by means of additives such as ettringite and/or gas generation.<sup>(6)</sup> Therefore, a competition between autogenous shrinkage and autogenous expansion occurs. In this regard, it is interesting to note that some of the curves were basically flat during the first few hours after initial set, as in the cases of the G2 and G3 grouts, which suggests a balance between expansion and contraction, not an absence of both. This is a desirable attribute for these grouts, but as evidenced by the illusory nature of this attribute for these and other grouts, it is clear that maintaining dimensional stability during setting and curing is a challenge. In the case of non-cementitious grouts (F1 and M1), the autogenous deformation was practically constant throughout the test. This might be attributed to the different type of chemical reaction taking place in these systems. Their chemical reaction might not involve any volume reduction (chemical shrinkage) at all. In the case of F1, the expansion observed might be attributed to some thermal effects associated to the reactions.

Special interest is given to the reason why some of the cement-based grouts expanded. As mentioned before, the first expansion and subsequent shrinkage might be due to expansive reactions such as the formation of ettringite (and, in lesser degree, to small thermal effects). Then, when the ettringite is later converted to monosulfate or monocarbonate phases, the stress producing the expansion might be released, and the specimen would shrink back toward its former state. This has been confirmed with SEM images as shown in figure 19. Additional autogenous shrinkage tests were being performed during the preparation of this report where some (inert) limestone particles were added to try to stabilize the ettringite formed at early ages and eliminate some of the later age autogenous shrinkage. Preliminary results show a reduction of the subsequent autogenous shrinkage. It is then conjectured that this shrinkage was due not to self-desiccation but rather to the loss of restraint as ettringite needles dissolved and were converted into monosulfate. While the main scope of the current research is to simply evaluate volume stability in grout-type materials, other research efforts are currently underway to facilitate a better characterization of the grouts so that the shrinkage results can be further explained from a fundamental basis. For instance, quantitative x-ray diffraction over time as well as isothermal calorimetry is being used to give some indication of what is happening chemically.



Note: conversion involved chemical shrinkage.

**Figure 19. Photo. Representative SEM images of the G3 grout: predominant ettringite (needle-shape) phase formation in the matrix at 2 d of hydration.**

### Long-Term Sealed and Drying Deformations (ASTM C157)

Long-term autogenous shrinkage (up to 6 mo) has been measured by means of the ASTM C157 test method.<sup>(2)</sup> The four sides of 1- by 1- by 12-inch (25- by 25- by 305-mm) prismatic specimens were sealed, and the length change was monitored. The results are presented in figure 21. Autogenous shrinkage obtained using the corrugated tubes and the (sealed) ASTM C157 test procedure was compared during the first 7 d, resulting in similar deformations in all cases, as shown in figure 20 for the G3 grout. This was also previously demonstrated by Sant et al.<sup>(44)</sup> Therefore, sealed specimens can be used with ASTM C157 to determine long-term autogenous shrinkage. All the curves in figure 21 start at 1 d and have been plotted so as to initiate at the corresponding strain values measured with the ASTM C1698 corrugated tubes test at 1 d for each of the grouts.<sup>(3)</sup> The largest values of sealed shrinkage after 184 d of reaction (about 500 to 700  $\mu\epsilon$ ) were observed for the cementitious grouts (G2, G3, and G4). The large initial expansion observed in G1 helped in reducing the final shrinkage value to about 200  $\mu\epsilon$ . The other two cementitious materials (G5 and U3) showed reduced shrinkage values (in the order of 300  $\mu\epsilon$ ), although those were still large values considering that the materials are maintained in sealed conditions. These values are similar to those obtained for the epoxy-based grouts (E1 and E2). On the other hand, M1 showed very low values of shrinkage (about 50  $\mu\epsilon$ ), and F1 depicted a net expansion (positive deformation) of about 50  $\mu\epsilon$  throughout the test duration. M2 could not be tested due to setting time limitations.

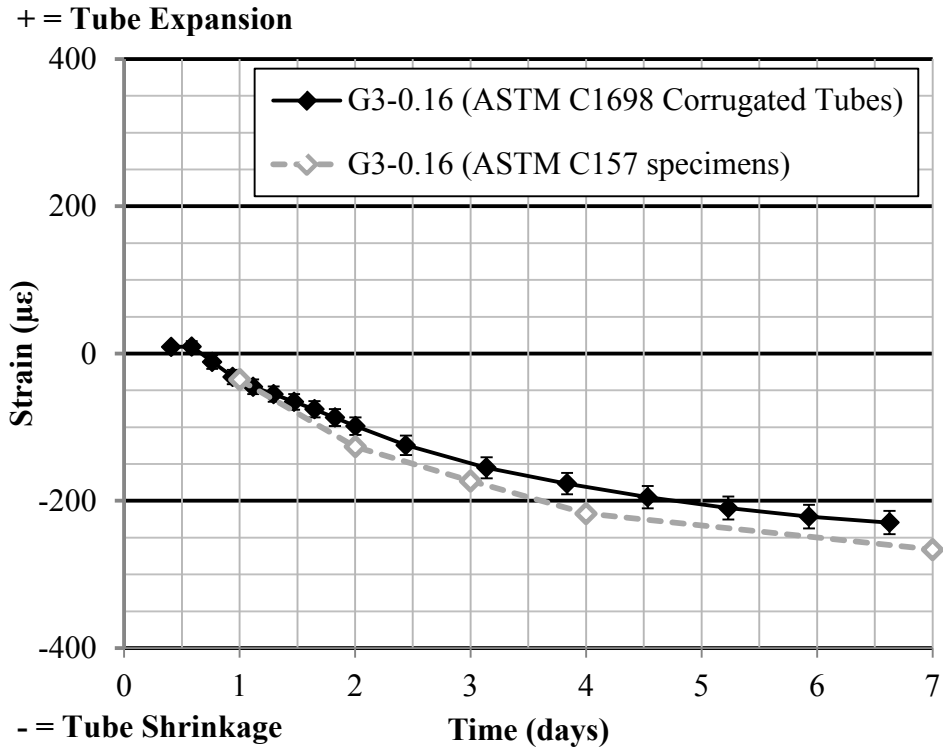
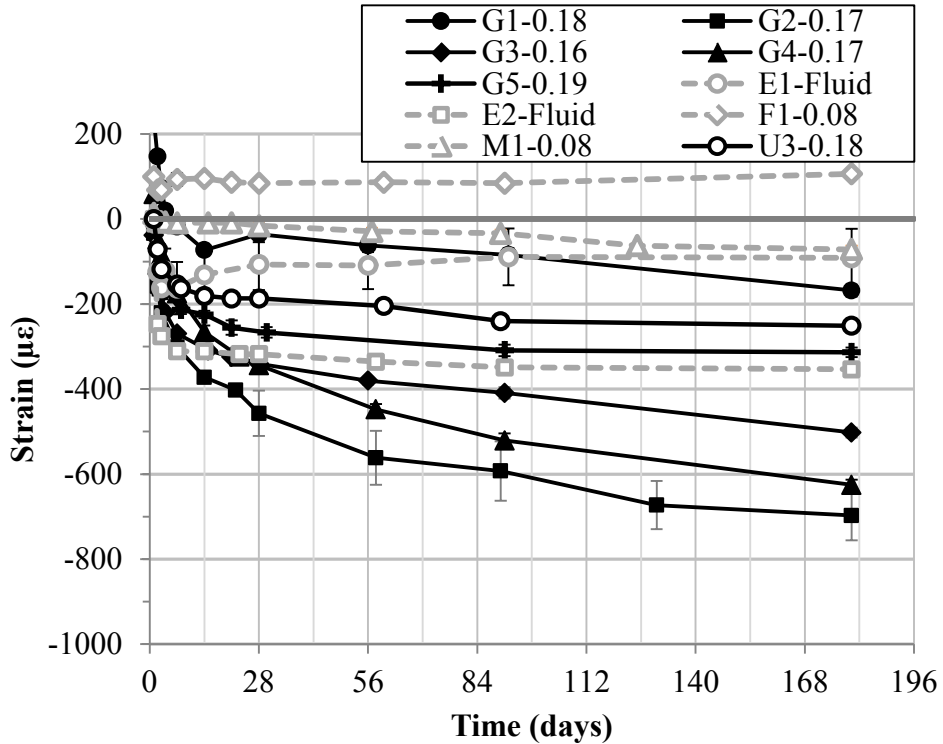


**Figure 20. Graph. Comparison of autogenous shrinkage results obtained using the ASTM C1698 corrugated tubes and the ASTM C157 sealed specimens.<sup>(3,2)</sup>**

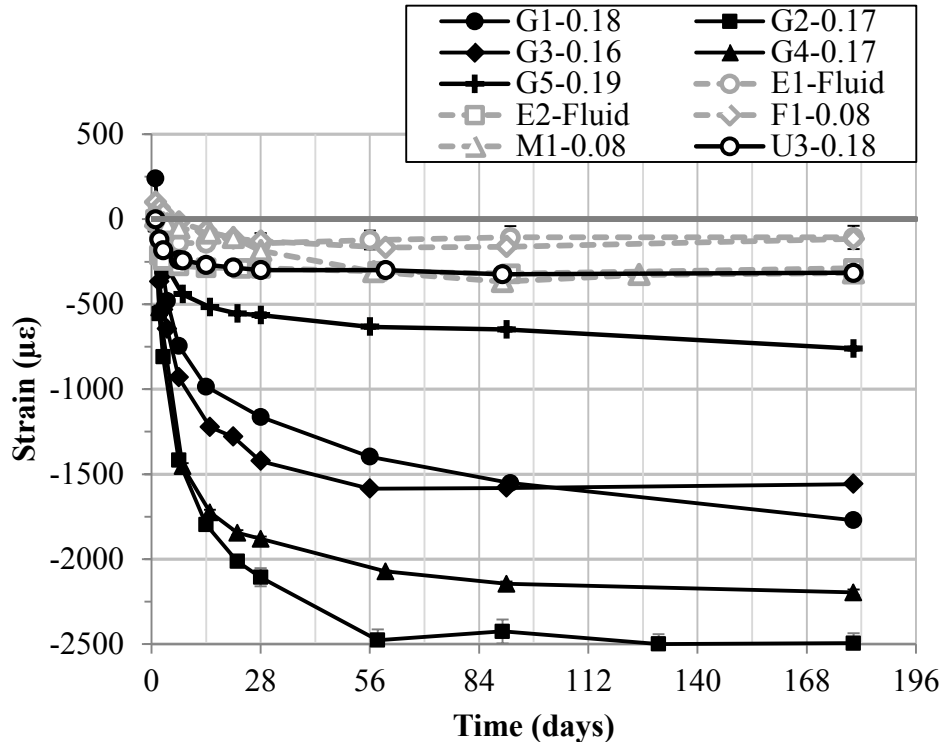




Note: error bars indicate one standard deviation as determined for four replicate specimens.

**Figure 21. Graph. Long-term autogenous (sealed) shrinkage as a function of time.**

Other specimens were also maintained in drying conditions at  $50 \pm 5$  percent RH to evaluate drying shrinkage (figure 22). Again, the curves start at 1 d and have been plotted so as to initiate at the corresponding strain values measured with the ASTM C1698 corrugated tubes test at 1 d for each of the grouts.<sup>(3)</sup> It is evident that the drying effect increased shrinkage in the cementitious materials (G1 through G4) by at least  $1,000 \mu\epsilon$ . Note that y-axis scale is different from that in figure 21. The increase in shrinkage is also evident in the G5 grout by about  $400 \mu\epsilon$ . Similarly, there was an increase in the shrinkage measured for the F1 and M1 materials with respect to sealed conditions. In this case, shrinkage values of about 50 and  $300 \mu\epsilon$  were observed, respectively. Finally, it is interesting to note that E1, E2, and U3 showed approximately the same amount of shrinkage as was observed in sealed conditions. M2 could not be tested due to setting time limitations.



Note: error bars indicate one standard deviation as determined for four replicate specimens.

**Figure 22. Graph. Long-term drying shrinkage as a function of time.**

### Discussion of Results

When focusing on the cement-based grouts (G1–G4), it is interesting to note that three of them (G2, G3, and G4) showed a considerable amount of shrinkage (approximately 500 to 700  $\mu\epsilon$ ) considering that they were cured in sealed conditions (see figure 21). The large initial expansion observed in G1 (see figure 18) helped in reducing most of its final shrinkage (about 200  $\mu\epsilon$ ). However, prior research has demonstrated that the rate of shrinkage (i.e., the slope of the autogenous shrinkage response) and the differential shrinkage are more critical parameters than the final shrinkage value when considering whether a material is prone to shrinkage cracking.<sup>(46)</sup> The drying results for these cementitious grouts show that drying shrinkage was at least 1,000  $\mu\epsilon$  larger than sealed shrinkage due to the additional drying effect contributing to shrinkage. Drying shrinkage is typically dependent on the water content (i.e., w/c or w/b). The higher the w/b, the larger the capillary pores, the faster they will dry out. This might be the case in these cement-based grouts, as the drying shrinkage values are high.

The two epoxy grouts used in this research show lower shrinkage values (100 to 400  $\mu\epsilon$ ) regardless of the curing condition. The reaction that occurs in this type of grout might undergo very small volume changes. Similarly, the UHPC used (U3) showed considerably lower shrinkage in both sealed and drying conditions (about 200  $\mu\epsilon$ ) compared with the cement-based grouts, despite being a cementitious material. It is interesting to note that U3 depicted larger autogenous shrinkage in the corrugated tube test during the first 7 d compared with the other cement-based grouts (see figure 18). As a reminder, the corrugated tube test was performed

without steel fibers. This is a good indication that the steel fibers typically included in the U3 mixture design contribute to eliminating some of the shrinkage taking place in the system.

As for the repair materials used (G5, F1, and M1), they showed lower shrinkage values than cement-based grouts and similar values to the epoxy grouts and the UHPC. Among them, G5 seemed to have larger values of shrinkage (about 800  $\mu\epsilon$  in drying conditions) due presumably to its cementitious nature. However these values are still much lower than the cement-based grouts. Finally, F1 and M1 did not depict any autogenous shrinkage after 6 mo, and their drying shrinkage values were very low (in the order of 300  $\mu\epsilon$ ), possibly due to similar reasons as in the case of epoxy grouts wherein the reaction that occurs in these materials might be associated with very small volume changes.

### **Preliminary Dimensional Stability Conclusions**

Based on the dimensional stability results obtained with the ASTM test methods recommended by ASTM C1107, the grouts selected in this study comply with this standard in terms of expansion.<sup>(1)</sup> However, some of the grouts showed a certain degree of height reduction that could presumably be referred to as shrinkage; however, the presence of other parameters (e.g., settlement) might lead to a misinterpretation of these results. A more fundamental approach must then be taken in order to understand whether this height reduction is due mainly to shrinkage deformations or not, and this was done by measuring pure expansion/shrinkage deformations as described by ASTM C1698 and by ASTM C157 in both sealed and drying conditions.<sup>(3,2)</sup> The results obtained in these tests show, contrary to what was previously mentioned, that all of the tested cementitious grouts undergo shrinkage at some point (in some cases, preceded by a small expansion), especially in drying conditions. This is an important finding because there appears to be a widely held misunderstanding of the performance of these “non-shrink” cementitious grouts. This misinterpretation of performance could lead to inappropriate expectations for the performance of these materials, particularly when used in connections for PBEs.

On the other hand, the two epoxy grouts, along with the repair materials and UHPC used in this research, underwent low shrinkage in both sealed and drying conditions. The relative dimensional stability of these materials could provide a significant advantage when deployed in connections between prefabricated concrete elements.

### **Appropriateness of ASTM C1107 Tests Methods to Evaluate Dimensional Stability**

As already mentioned, ASTM C1107 references two other ASTM test methods to evaluate dimensional stability in grouts.<sup>(1)</sup> These are ASTM C827 (for fresh-stage height changes) and ASTM C1090 (for hardened-stage height changes).<sup>(39,40)</sup> Each of these tests was observed to deliver results that do not provide a complete picture of the dimensional stability of the tested materials.

A modified version of the ASTM C827 was previously proposed and used in this research for several reasons.<sup>(41)</sup> The original setup of this test (i.e., projector lamp, magnifying lens, and indicator charts) is time-consuming because of the need to manually record the increase/decrease in specimen height. The test also shows a clear propensity toward human error as it is difficult to

clearly define the edge of the ball on the indicator charts since the shadow loses focus as the ball moves up or down. Another issue of using the original setup described in ASTM C827 is that the cylindrical specimen is not completely unrestrained.<sup>(39)</sup> As previously mentioned, there is always a certain degree of friction between the specimen's sides and the inner surface of the metallic mold. This is why, in order to provide the lowest friction possible, an acetate sheet was used between the test specimen and the mold. Although not shown in this report, specimens were also prepared without the acetate sheet, with results showing slightly smaller height changes (increase or decrease), due to a slight increase in the degree of restraint. Thermal effects (normally expansion) could also be assessed by measuring the temperature of the test specimen throughout the test.

As for ASTM C1090, this test method has the previously mentioned shortcoming of not allowing the specimens to expand during the first hours of the material's properties development due to the presence of the glass plate.<sup>(40)</sup> Another issue is that it is sometimes difficult to remove the glass plate from the top surface of the specimen, especially when using grout-type materials as opposed to cement-based materials (e.g., epoxy-resinous). This problem can be resolved by using a piece of acetate sheet in between the glass plate and the top surface of the specimen. It is also recommended to use acetate sheet to reduce most of the friction (i.e., restraint) between the specimen and the mold.

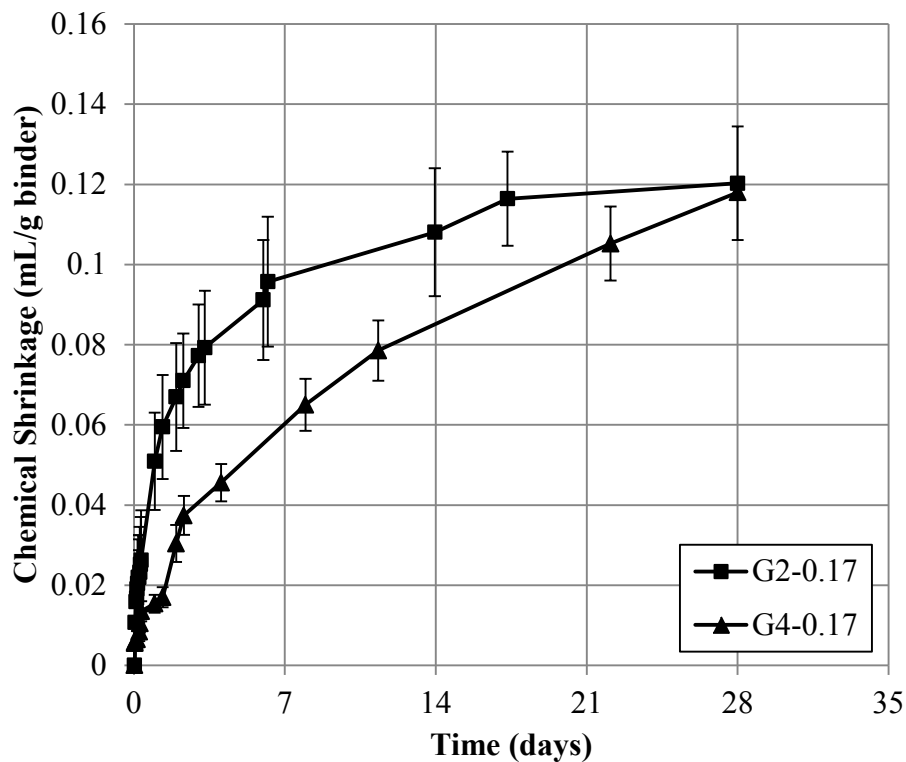
Common shortcomings for both of these test methods include the consideration of the simultaneous occurrence of several parameters (expansion, chemical and autogenous shrinkage, surface settlement, plastic shrinkage, etc.). Due to the presence of all these parameters, the measurements are more useful for comparative purposes but are less useful for quantitative assessment of shrinkage or expansion propensity. In addition, none of these test methods assess drying shrinkage, which has been shown to be a major component of the overall shrinkage. While ASTM C1090 is executed in sealed conditions, ASTM C827 only allows for a small exposed surface area and thus a reduced drying shrinkage component.<sup>(40,39)</sup> Finally, both standards could benefit from increased clarity in their definition of shrinkage and expansion limits within particular timeframes. For instance, in the case of using the ASTM C827 test method, a mixture could expand more than 4 percent during its fresh stage and return to a value below 4 percent before reaching final set, thus apparently still meeting the standard.<sup>(39)</sup>

## **IC TECHNOLOGY**

### **Chemical Shrinkage for IC Design**

Because all cementitious grouts used in this research showed shrinkage, it was decided that two of them could be modified so that IC was included. This was done using prewetted LWAs at a dosage calculated using the equation in figure 3. As already mentioned, grouts are sometimes extended with normal weight aggregates, commonly for castings with dimensions of 6 inches (152.4 mm) or more. IC can be thought of as an extension of the grouts using prewetted LWA rather than normal weight aggregate. The idea behind using IC is to improve dimensional stability by reducing shrinkage, especially during the first days when the tensile strength of the material is still low. One of the terms needed for using figure 3 is the chemical shrinkage of the reactive fraction of the solid of each grout. Therefore, chemical shrinkage measurements for two of the cement-based grouts are presented in figure 23. The chemical shrinkage results are

typically normalized by grams of binder (reactive material). As observed, both grouts provided the same amount of chemical shrinkage after 28 d of measurements. However, it is evident that G4 showed a higher rate of chemical shrinkage during the latter half of the timeframe, as indicated by the slope of the curve. This might be due to the estimated larger amount of reactive material in this grout as compared with that of G2 (see Mixture Proportioning with IC section in chapter 3). This is in agreement with the petrographic analysis in which the amount of measured reactive material of G2 and G4 was approximately 30 and 35 percent, respectively. By plotting the chemical shrinkage results as a function of the inverse of the time, it is possible to estimate the infinite chemical shrinkage needed for figure 3. This was done, and values of 1.99 and 2.15 fl oz/lb (0.13 and 0.14 mL/g) binder were obtained for G2 and G4, respectively, which again is in agreement with the larger amount of reactive material present in G4 based on the petrographic analysis. In other words, the G4 grout needs more prewetted LWA due to the larger infinite chemical shrinkage compared with G2 (see table 3).



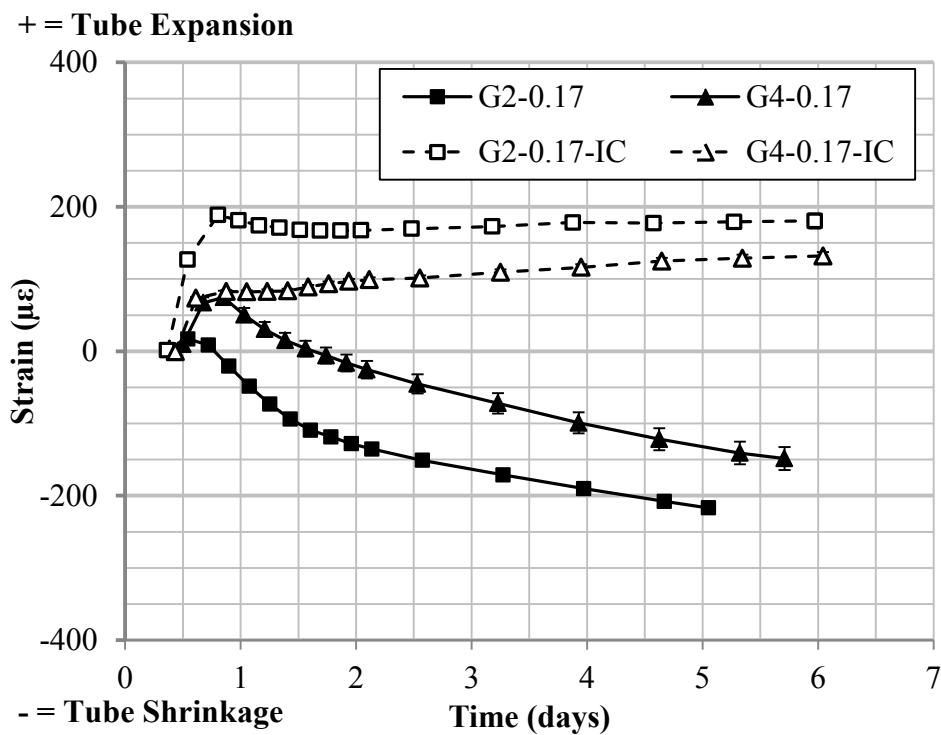
1 fl oz/lb = 0.065 mL/g  
 Note: error bars indicate one standard deviation of three replicate specimens.

**Figure 23. Graph. Chemical shrinkage as a function of time of two of the cement-based grouts.**

### Autogenous and Drying Deformations with IC

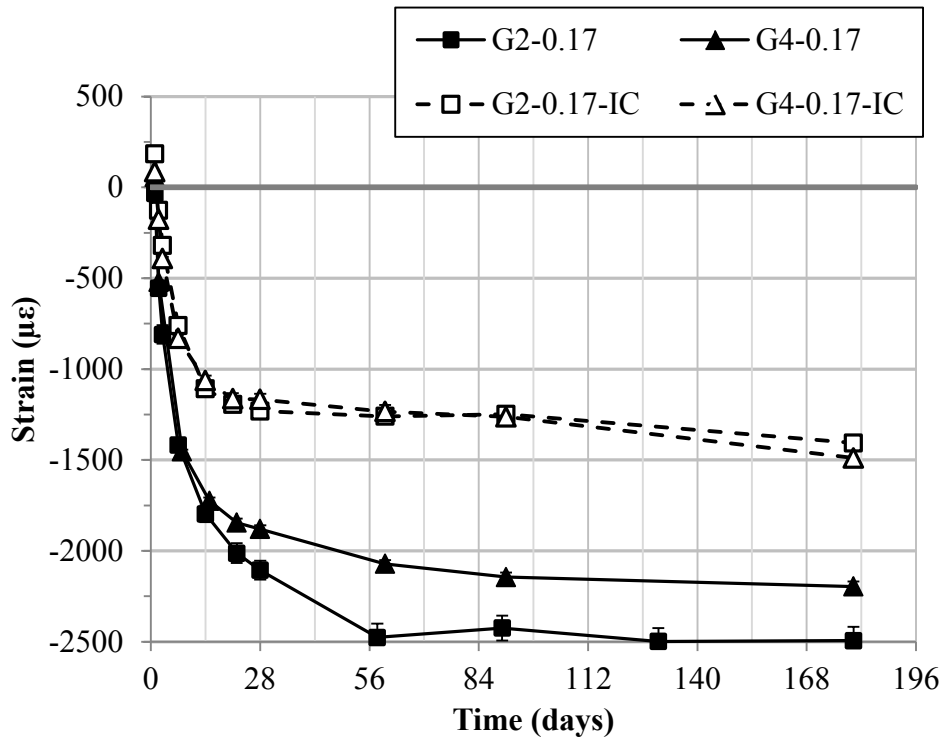
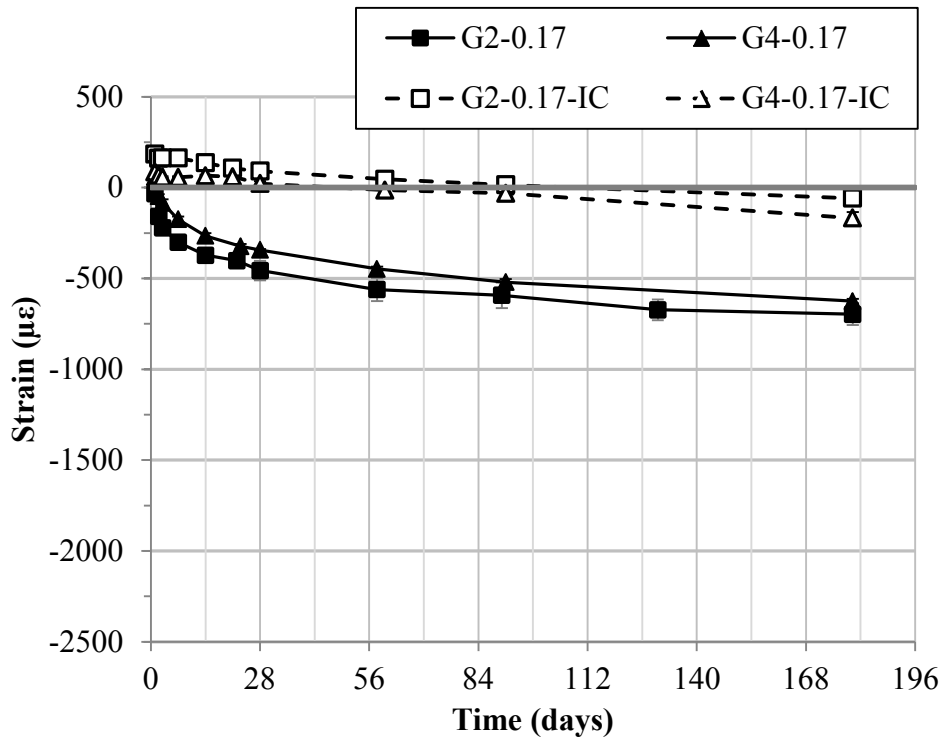
Both autogenous and drying shrinkage were measured in the two cement-based grouts where IC was included. The results are shown in figure 24 (autogenous shrinkage via corrugated tubes test) and figure 25 (long-term autogenous and drying shrinkage).

When IC was added, the autogenous shrinkage component was removed, and the “true” expansive nature of the binder was revealed, as shown in figure 24. Long-term results are presented in figure 25. Again, the curves start at 1 d and have been zeroed to the corresponding strain measured with the corrugated tubes test at 1 d for each of the grouts. As can be observed, IC totally eliminates autogenous shrinkage during the first days of hydration reaction, resulting instead in a small autogenous expansion, perhaps due to ettringite formation and/or swelling of the cement hydration products due to water absorption. Less drying shrinkage is also observed despite their higher overall water content and greater mass loss during drying. The partial reduction would presumably correspond to two different reasons: (1) mitigation of autogenous (or internal) drying, and (2) extension in the time it takes to reach equilibrium with the local drying environment, because it may take longer to empty out the same-sized pores in the system with IC versus the system without IC.



Note: error bars indicate one standard deviation as determined for three replicate specimens.

**Figure 24. Graph. Effect of IC on the autogenous shrinkage.**



Note: error bars indicate one standard deviation as determined for four replicate specimens.

**Figure 25. Graph. Effect of IC on the long-term autogenous (sealed) shrinkage (top) and long-term drying shrinkage (bottom) as a function of time.**

## Compressive Strength with IC

The inclusion of prewetted LWA to provide IC was not expected to reduce the strength development of the grouts. In fact, other research has reported increases in the strength development at later ages, presumably due to an increase in the degree of hydration as well as the formation of a finer microstructure.<sup>(23)</sup> The effect that IC has on the strength development of the grouts used in this study is presented in table 9. IC clearly increases the strength in the G2 grout and maintains it in the case of G4. The reason for the different strength development of the two internally cured grouts is not clear because they are proprietary materials with unknown formulations. Normally, IC would increase the degree of hydration of the system; however, this parameter was not measured. Nevertheless, these two grouts have shown enough early strength with or without IC so that the strength requirements in ASTM C1107 are fulfilled.<sup>(1)</sup>

**Table 9. Effect of IC on the compressive strength.**

Grout	Average Compressive Strength, psi			
	1 d	3 d	7 d	28 d
G2 - 0.17	5,018 (110) <sup>a</sup>	7,150 (220)	8,833 (10)	9,805 (220)
G2 - 0.17 - IC	4,540 (51)	7,469 (41)	10,182 (141)	13,010 (511)
G4 - 0.17	2,408 (51)	3,800 (110)	5,149 (30)	6,338 (59)
G4 - 0.17 - IC	2,016 (20)	3,989 (30)	4,902 (351)	5,961 (231)

1 psi = 0.007 MPa

<sup>a</sup>Numbers in parentheses indicate one standard deviation in psi as determined for three replicate specimens tested at each age.

## Additional Cost to Include IC

Besides reducing the autogenous and drying shrinkage, IC can also bring cost benefits because the cost per yielded volume of LWA is less than the cost per yielded volume of grout (solid fraction).<sup>2</sup> The mix designs for the IC grouts are provided in table 3. As shown in the table, these two grouts yield approximately 20 percent more volume when extended with the prewetted lightweight fine aggregate to promote IC. In other words, when extending a grout with LWA to yield 1 yd<sup>3</sup> (0.76 m<sup>3</sup>) of material, the amount of solid grout needed is reduced, thus decreasing the overall material unit cost. Reduction in the cost per (internally cured) grout yielded volume has been estimated at about 20 to 25 percent for the grouts used in this research study. This cost reduction does not consider deployment costs.

---

<sup>2</sup>Bulk unit cost of the LWA used in this study is approximately \$60/T.



## CHAPTER 5. CONCLUSIONS AND RECOMMENDATIONS

### SUMMARY

The research presented in this report focuses on addressing performance concerns related to dimensional stability (primarily early age shrinkage) of commonly used grouts. Some grouts, many of which are classified as “non-shrink grouts,” have been observed to display significant dimensional instability when deployed in connection details during bridge construction projects. ASTM C1107, the test method commonly used to assess the dimensional stability of these grouts, has been observed to deliver an incomplete picture of the overall performance.<sup>(1)</sup> This research demonstrates the types of performance that can be expected from these types of grouts, the shortcomings of the commonly used test methods, and alternative test methods that may better demonstrate real-world performance.

The general approach followed in this research was to first evaluate the dimensional stability of 11 commercially available grout-type materials following the guidelines described in the ASTM C1107 test method.<sup>(1)</sup> After an initial evaluation, it was observed that the tests methods used for evaluating dimensional stability described in this standard specification consider several parameters simultaneously (e.g., thermal expansion, chemical expansion, chemical shrinkage, autogenous shrinkage, plastic shrinkage, settlement, etc.), thus providing a qualitative approach that is only useful for comparative purposes. To more completely assess this variety of parameters, volume changes must be assessed from a fundamental point of view, measuring pure expansion/shrinkage deformations over time. As such, additional tests to evaluate the dimensional stability of the grouts were used (e.g., ASTM C157 and ASTM C1698).<sup>(2,3)</sup> Finally, given the fact that these grouts commonly exhibit shrinkage, this research also included additional tests focused on the partial shrinkage mitigation by including IC in some of the cement-based grouts.

### CONCLUSIONS AND RECOMMENDATIONS

Based on the results obtained, the following conclusions can be drawn:

- Most of the cement-based grouts evaluated in this research (G1–G4) seemed to perform well in terms of dimensional stability when tested in accordance with ASTM C1107.<sup>(1)</sup> However, separate testing to assess autogenous and drying deformations (shrinkage and expansion) show that behaviors not captured by the test method can result in a lack of dimensional stability. These grouts tended to undergo expansion during the first day or two, followed by shrinkage, especially in drying conditions. It has been demonstrated that this expansion is typically dominated by the formation of ettringite phases. The subsequent shrinkage is due mainly to the conversion of the ettringite phase into monosulfate or monocarbonate phases, a reaction that involves chemical shrinkage. Part of the expansive behavior of some of these grouts is also attributed to the formation of gas within the matrix. Given that ASTM C1107 is a standard for defining nonshrink grouts, it is relevant to raise awareness of the specific types of shrinkage and expansion that are captured by the standard.<sup>(1)</sup>

- In general terms, the other types of tested materials, including epoxy, magnesium phosphate, and fly-ash-based, showed improved performance compared with the cementitious grouts based on the lower autogenous and drying deformations obtained. These are G5, E1, E2, F1, M1, and M2. Although commonly marketed as repair materials, these materials can be used as grouts, according to the materials' suppliers, due to their high initial flowability and early-age strength development. These materials barely showed shrinkage or dimensional instability, which makes them proper materials for applications where dimensional stability is a strong requirement. Note that limited results were obtained for M2 due to the very short setting times (about 5 min). Also, the ASTM test methods used in this research for assessing volume changes in cementitious grouts can present some difficulties when testing some non-cement-based grouts such as the ones used in this research.
- IC (through the use of prewetted LWAs) seemed to mitigate most of the autogenous shrinkage and reduced the drying shrinkage in the two cement-based grouts tested by half. This might be a good option for cementitious grouts, considering that other benefits might be provided (increased strength and durability, reduced transport, more compliant material with a lower cracking propensity, etc.). The implementation of the IC technology as a grout extension can be helpful not only in reducing shrinkage but also in improving curing conditions in some locations where conventional (external) curing is difficult or impossible to implement. This technology would also provide some robustness to the surface preparation (in terms of moisture content) of the precast (or existing) concrete elements because prewetted LWA may also serve as additional reservoirs if water is drawn from the grout into the substrate.
- Both ASTM C827 and ASTM C1090 test methods present a series of shortcomings that should be further considered when evaluating dimensional stability of grout-type materials, the main one being that both methods consider the simultaneous occurrence of several parameters that affect dimensional stability (e.g., surface settlement).<sup>(39,40)</sup> This allows for a qualitative performance comparison, rather than for a quantitative assessment of shrinkage and expansion propensity. The experimental details in the test also present shortcomings. For instance, the current version of the ASTM C827 test method is time-consuming and prone to human error. As an alternative, a different setup was used in the presented research study. Other method limitations were previously described in the report.
- Material cost should be considered in the evaluation. While non-cement-based grouts are typically more expensive than cement-based grouts (up to four times more expensive, in some cases), they show higher strength development and fewer volume changes. Cement-based grouts are widely used due to their lower cost. If cement-based grouts are extended with prewetted LWA to include IC, then their initial cost could decrease while their performance could benefit.

The authors of the study recommend the use of modified and alternative ASTM test methods to better characterize the dimensional stability performance of grout-type materials. As shown in the study, some grout materials may seem to fulfill the volume stability requirements defined by the ASTM C1107 test method.<sup>(1)</sup> However, further evaluation shows a considerable amount of

shrinkage in most of the grouts tested. The misinterpretation of performance could lead to an improper use of these materials, which would have an impact in the general performance of these materials when used as connections for PBEs.

In addition, IC is recommended as a convenient strategy to reduce shrinkage deformations and, consequently, shrinkage cracking. The inclusion of IC in pre-bagged grout materials could easily be implemented in the field as a grout extension or even as part of the premix material. This would also facilitate curing operations, especially in difficult-to-access locations.

## **ONGOING AND FUTURE RESEARCH**

The assessment of the dimensional stability is an early step in evaluating the propensity for shrinkage and thermal cracking of these materials. Other tests need to be performed where a certain degree of restraint is provided so that the material would indeed crack, thus evaluating the cracking resistance of the material. In this regard, the commonly known dual ring test would be a good candidate for evaluating the autogenous and thermal cracking capacity of these materials because some of them (especially the repair materials) release a high amount of heat during their reaction that might cause not only shrinkage stresses but also thermal stresses.<sup>(47)</sup> In addition, other material properties that have influence on the cracking resistance should also be assessed, including tensile strength, elastic modulus, and tensile creep.

It is also important to mention that dimensional instability will theoretically have an influence on the bond performance of these materials. This is of special importance in the type of applications where these materials are expected to be used (i.e., connections for prefabricated concrete elements). Research is currently underway to investigate the correlation between dimensional stability and bonding of grouts to precast concrete.

Finally, research is also needed to further optimize the IC design in grout-type materials. For instance, an overdose of prewetted LWA in the system could be detrimental from the durability point of view. The addition of LWA has also been observed to potentially reduce the fresh flowability of cement-based grouts. As an alternative, SAP might be an option worthy of evaluation.



## **APPENDIX A. MANUFACTURER REPORTED GROUT PERFORMANCE INFORMATION**

Table 10 through table 13 summarize some of the material properties specified by the corresponding manufacturers. The properties shown were selected based on the relevance to this research study (e.g., dimensional stability, compressive strength, etc.).

**Table 10. Cement-based grouts.**

Grout Nomenclature		G1		G2			G3		G4	
Grout Description		Non-shrink, air entrained, non-metallic		Non-shrink, metallic			Non-shrink, air entrained, non-metallic		Non-shrink, air entrained, non-metallic	
Dimensional Stability in Terms of Height Change (Percent)	Early Height Change <sup>(39)</sup>	0.0 to 4.0		a			0.68		0.0 to 4.0	
	Hardened Height Change <sup>(40)</sup>	0.0 to 0.3		0.0 to 0.08			0.0 to 0.06		0.0 to 0.3	
Dimensional Stability in Terms of Length Change (Percent) <sup>(2)</sup>	28 d	a		a			a		a	
Compressive Strength, psi (MPa) <sup>(36)</sup>	Consistency <sup>b</sup>	Min water	Max water	Plastic <sup>c</sup>	Flowable <sup>c</sup>	Fluid <sup>c</sup>	Plastic <sup>d</sup>	Flowable <sup>d</sup>	Min water	Max water
	1 d	4,000 (27.6)	2,500 (17.3)	5,000 (34.5)	5,000 (34.5)	4,000 (27.6)	4,400 (30.3)	2,400 (16.5)	5,800 (27.6)	3,500 (24.2)
	3 d	5,500 (38.0)	3,500 (24.1)	7,000 (48.3)	6,000 (41.4)	5,000 (34.5)	a	a	7,500 (51.7)	6,000 (41.4)
	7 d	6,500 (44.8)	5,000 (34.5)	9,000 (62.1)	8,000 (55.2)	7,000 (48.3)	7,800 (53.8)	6,400 (44.1)	8,000 (55.2)	6,500 (44.8)
	28 d	8,000 (55.2)	6,500 (44.8)	11,000 (75.8)	10,000 (68.9)	9,000 (62.1)	9,000 (62.1)	7,600 (52.4)	10,000 (68.9)	8,000 (55.2)

<sup>a</sup>Not reported.

<sup>b</sup>Strength will vary based on amount of water used to mix the pre-blended dry components (i.e., consistency).

<sup>c</sup>Consistency nomenclature based on ASTM C1107.<sup>(1)</sup>

<sup>d</sup>Consistency nomenclature based on New York State Department of Transportation 701-05 and 701-06.<sup>(48,49)</sup>

**Table 11. Repair materials.**

Grout Nomenclature		G5	F1 <sup>a</sup>	M1 <sup>b</sup>	M2
Grout Description		Cement-based	Fly ash-based	Magnesium phosphate-based	Magnesium phosphate-based
<b>Dimensional Stability in Terms of Height Change (Percent)</b>	<b>Early Height Change<sup>(39)</sup></b>	c	c	c	c
	<b>Hardened Height Change<sup>(40)</sup></b>	c	c	c	c
<b>Dimensional Stability in Terms of Length Change (Percent)<sup>(2)</sup></b>	<b>28 d</b>	c	< 0.020 (dry)	c	-0.0085 (soak) -0.0595 (dry)
<b>Compressive Strength, psi (MPa)<sup>(36)</sup></b>	<b>1 h</b>	3,300 (22.8)	c	c	c
	<b>2 h</b>	c	> 2,500 (> 17.2)	c	> 2,500 (> 17.2)
	<b>3 h</b>	4,800 (33.1)	c	3,000 (20.7)	> 3,500 (> 24.1)
	<b>6 h</b>	c	c	5,000 (34.5)	c
	<b>1 d</b>	6,500 (44.8)	> 5,000 (> 34.5)	6,000 (41.4)	> 4,000 (> 27.6)
	<b>3 d</b>	c	c	7,000 (48.3)	c
	<b>7 d</b>	c	> 6,000 (> 41.4)	c	> 5,000 (> 34.5)
<b>28 d</b>	9,500 (65.5)	> 7,000 (> 48.3)	8,500 (58.6)	> 6,000 (> 41.4)	

<sup>a</sup>Strength measured using 4-inch (101.6-mm)-diameter by 8-inch (203.2-mm)-height cylinders.<sup>(50)</sup>

<sup>b</sup>Strength measured at a temperature of 95 °F (35 °C).

<sup>c</sup>Not reported.

**Table 12. Epoxy-based grouts.**

Grout Nomenclature		E1		E2	
Grout Description		Three-component, expansive, non-shrink		Three-component, expansive, non-shrink	
Dimensional Stability in Terms of Height Change (Percent)	Early Height Change <sup>(39)</sup>	Positive expansion		Positive expansion	
	Hardened Height Change <sup>(40)</sup>	a		a	
Dimensional Stability in Terms of Length Change (Percent) <sup>(2)</sup>	28 d	a		a	
Compressive Strength, psi (MPa) <sup>(51)</sup>	Consistency	Standard	High flow	Standard	High flow
	16 h	11,000 (75.8)	10,000 (68.9)	a	a
	1 d	15,000 (103.4)	14,000 (96.5)	11,000 (75.8)	9,000 (62.1)
	7 d	16,500 (113.8)	16,000 (110.3)	14,000 (96.5)	13,000 (89.6)
	Post-cured at 140 °F (60 °C)	17,500 (120.7)	17,000 (117.2)	15,500 (106.9)	14,500 (100.0)

<sup>a</sup>Not reported.



**Table 13. Ultra-high performance concrete.**

<b>Grout Nomenclature</b>		U3		
<b>Grout Description</b>		Cementitious-based, steel fiber-reinforced		
<b>Dimensional Stability in Terms of Height Change (Percent)</b>	<b>Early Height Change<sup>(39)</sup></b>	a		
	<b>Hardened Height Change<sup>(40)</sup></b>	a		
<b>Dimensional Stability in Terms of Length Change (Percent)<sup>(2)</sup></b>	<b>28 d</b>	a		
<b>Compressive Strength, ksi (MPa)<sup>(50)b</sup></b>	<b>Temperature, °F (°C)</b>	50 (10)	73 (23)	105 (41)
	<b>12 h</b>	0.5	2.0	13.0
	<b>1 d</b>	2.5	13.0	18.5
	<b>3 d</b>	13.0	17.0	20.5
	<b>7 d</b>	16.5	18.0	22.0
	<b>14 d</b>	18.0	21.5	23.0

<sup>a</sup>Not reported.

<sup>b</sup>Strength measured using 3-inch (76-mm)-diameter by 6-inch (152-mm)-height cylinders at a loading rate of 150 psi/s (1.0 MPa/s).<sup>(50)</sup>



## **ACKNOWLEDGMENTS**

The authors would like to thank Daniel Balcha for his technical assistance, Dr. José Muñoz for collecting SEM images, and Dr. Mengesha Beyene for his assistance in the petrographic analysis. Special thanks go to Dale Bentz for all his valuable comments. The research that is the subject of this document was funded by FHWA. This support is gratefully acknowledged.



## REFERENCES

1. ASTM C1107 (2014). *Standard Specification for Non-Shrink Packaged Dry, Hydraulic-Cement Grout*. ASTM International. West Conshohocken, PA.
2. ASTM C157 (2014). *Standard Test Method for Length Change of Hardened Hydraulic-Cement Mortar and Concrete*. ASTM International. West Conshohocken, PA.
3. ASTM C1698 (2014). *Standard Test Method for Autogenous Strain of Cement Paste and Mortar*. ASTM International. West Conshohocken, PA.
4. Ralls Newman, M.L. (2006). *Decision-Making Framework for Prefabricated Bridge Elements and Systems (PBES)*. Report No. FHWA-HIF-06-030. Federal Highway Administration. Washington, DC.
5. Ralls Newman, M.L. (2007). *Manual on Use of Self-Propelled Modular Transporters to Remove and Replace Bridges*. Report No. FHWA-HIF-07-022. Federal Highway Administration. Washington, DC.
6. Culmo, M.P. (2009). *Connection Details for Prefabricated Bridge Elements and Systems*. Report No. FHWA-IF-09-010. Federal Highway Administration. Washington, DC.
7. Vanderlans, G.J. (1983). *Sealing Device for Use in Grouting Pipe Joints and Method of Using Same*. U.S. Patent No. 4,421,698.
8. Weber, V. (1978). *Joint Sealing Method*. U.S. Patent No. 4,098,047.
9. Clarke, W.J. (1982). *Magnesium Diacrylate, Polyol Monoacrylate Grouting Composition and Method for Grouting Joints and/or Cracks in Sewer Conduits Therewith*. U.S. Patent No. 4,318,835.
10. McIntosh, J. and Sperling, N.C. (2009). *Modular Flooring Assemblies*. U.S. Patent No. 7,543,417.
11. Shannag, M.J. (2002). "High-Performance Cementitious Grouts for Structural Repair." *Cement and Concrete Research*, 32(5), 803–808.
12. Khayat, K.H. and Yahia, A. (1998). "Simple Field Tests to Characterize Fluidity and Washout Resistance of Structural Cement Grout." *Cement, Concrete and Aggregates*, 20(1), 145–156.
13. Allen, R.T.L. (1993). *The Repair of Concrete Structures*. S.C. Edwards, and J.D.N. Shaw (Eds.). Blackie Academic & Professional, London, England.
14. Gulyas, R.J., Wirthlin, G.J., and Champa, J.T. (1995). "Evaluation of Keyway Grout Test Methods for Precast Concrete Bridges." *PCI Journal*, 40(1), 44–57.

15. Issa, M.A., Anderson, R., Domagalski, T., Asfour, S., and Islam, M.S. (2007). "Full-Scale Testing of Prefabricated Full-Depth Precast Concrete Bridge Deck Panel System." *ACI Structural Journal*, 104(3), 324–332.
16. Ma, J. (2010). *Durability Performance Criteria of Closure Pour Materials for CIP Connections*. PCI Bridge Conference. Washington, DC.
17. Graybeal, B. (2013). *Material Characterization of Field-Cast Connection Grouts*. Report No. FHWA-HRT-13-042. Federal Highway Administration. Washington, DC.
18. Bentz, D.P. and Weiss, W.J. (2011). *Internal Curing: A 2010 State-of-the-Art Review*. U.S. Department of Commerce. National Institute of Standards and Technology. Gaithersburg, MD.
19. Kovler, K. and Jensen, O. (Eds.) (2007). *Internal Curing of Concrete*. Reunion Internationale des Laboratoires et Experts des Materiaux, Systemes de Construction et Ouvrages. Bagneux, France.
20. Roberts, J.W. (2005). "High Performance Concrete, Enhancement through Internal Curing." *Concrete InFocus*. National Ready Mixed Concrete Association, 55–57.
21. Cusson, D., Lounis, Z., and Daigle, L. (2010). "Benefits of Internal Curing on Service Life and Life-Cycle Cost of High-Performance Concrete Bridge Decks—A Case Study." *Cement and Concrete Composites*, 32(5), 339–350.
22. Zhutovsky, S., Kovler, K., and Bentur, A. (2002). "Efficiency of Lightweight Aggregates for Internal Curing of High Strength Concrete to Eliminate Autogenous Shrinkage." *Materials and Structures*, 35(2), 97–101.
23. De la Varga, I., Castro, J., Bentz, D., and Weiss, J. (2012). "Application of Internal Curing for Mixtures Containing High Volumes of Fly Ash." *Cement and Concrete Composites*, 34(9), 1,001–1,008.
24. Barrett, T.J., De la Varga, I., Schlitter, J., and Weiss, W.J. (2011). *Reducing the Risk of Cracking in High Volume Fly Ash Concrete by Using Internal Curing*. World of Coal Ash Conference, Denver, CO.
25. De la Varga, I., Spragg, R.P., Di Bella, C., Castro, J., Bentz, D.P., and Weiss, J. (2014). "Fluid Transport in High Volume Fly Ash Mixtures with and without Internal Curing." *Cement and Concrete Composites*, 45, 102–110.
26. Bentz, D.P., Lura, P., and Roberts, J.W. (2005). "Mixture Proportioning for Internal Curing." *Concrete International*, 27(2), 35–40.
27. ASTM C1608 (2012). *Standard Test Method for Chemical Shrinkage of Hydraulic Cement Paste*. ASTM International. West Conshohocken, PA.

28. ASTM C1761 (2015). *Standard Specification for Lightweight Aggregate for Internal Curing of Concrete*. ASTM International. West Conshohocken, PA.
29. Graybeal, B.A. (2006). *Material Property Characterization of Ultra-High Performance Concrete*. Publication No. FHWA-HRT-06-103. Federal Highway Administration. Washington, DC.
30. Graybeal, B.A. (2009). "UHPC Making Strides." *Public Roads*, 72(4), 17–21.
31. Graybeal, B. (2011). *Ultra-High Performance Concrete*. Report No. FHWA-HRT-11-038. Federal Highway Administration. Washington, DC.
32. ASTM C1437 (2013). *Standard Test Method for Flow of Hydraulic Cement Mortar*. ASTM International. West Conshohocken, PA.
33. ASTM C231 (2014). *Standard Test Method for Air Content of Freshly Mixed Concrete by the Pressure Method*. ASTM International. West Conshohocken, PA.
34. ASTM C138 (2014). *Standard Test Method for Density (Unit Weight), Yield, and Air Content (Gravimetric) of Concrete*. ASTM International. West Conshohocken, PA.
35. ASTM C403 (2008). *Standard Test Method for Time of Setting of Concrete Mixtures by Penetration Resistance*. ASTM International. West Conshohocken, PA.
36. ASTM C109 (2013). *Standard Test Method for Compressive Strength of Hydraulic Cement Mortars (Using 2-in. or [50-mm] Cube Specimens)*. ASTM International West Conshohocken, PA.
37. ASTM C1679 (2014). *Standard Practice for Measuring Hydration Kinetics of Hydraulic Cementitious Mixtures Using Isothermal Calorimetry*. ASTM International. West Conshohocken, PA.
38. Le Chatelier, H. (1900). *Sur les Changements de Volume qui Accompagnent le durcissement des Ciments*. Bulletin Societe de l'Encouragement pour l'Industrie Nationale, Seme serie, tome 5, Paris, France.
39. ASTM C827 (2010). *Standard Test Method for Change in Height at Early Ages of Cylindrical Specimens of Cementitious Mixtures*. ASTM International. West Conshohocken, PA.
40. ASTM C1090 (2010). *Standard Test Method for Measuring Changes in Height of Cylindrical Specimens of Hydraulic-Cement Grout*. ASTM International. West Conshohocken, PA.
41. Di Bella, C. and Graybeal, B.A. (2014). "Volume Stability and Cracking Potential of Prebagged, Cement-Based Nonshrink Grouts for Field-cast connections." *Transportation Research Record: Journal of the Transportation Research Board*, 2441(1), 6–12.

42. Powers, T.C. and Brownyard, T.L. (1946). "Studies of the Physical Properties of Hardened Portland Cement Paste." *ACI Journal Proceedings*, 43(9), 249–336.
43. Lura, P., Jensen, O.M., and van Breugel, K. (2003). "Autogenous Shrinkage in High-Performance Cement Paste: An Evaluation of Basic Mechanisms." *Cement and Concrete Research*, 33(2), 223–232.
44. Sant, G., Lura, P., and Weiss, J. (2006). "Measurement of Volume Change in Cementitious Materials at Early Ages: Review of Testing Protocols and Interpretation of Results." *Transportation Research Record: Journal of the Transportation Research Board*, 1979(1), 21–29.
45. Cusson, D. (2008). "Effect of Blended Cements on Effectiveness of Internal Curing of HPC." *ACI SP-256: Internal Curing of High-Performance Concretes: Laboratory and Field Experiences*, 105–120.
46. Shah, H.R. and Weiss, J. (2006). "Quantifying Shrinkage Cracking in Fiber Reinforced Concrete Using the Ring Test." *Materials and Structures*, 39(9), 887–899.
47. Schlitter, J.L., Senter, A.H., Bentz, D.P., Nantung, T., and Weiss, W.J. (2010). "Development of a Dual Ring Test for Evaluating Residual Stress Development of Restrained Volume Change." *Journal of ASTM international*, 7, 13.
48. New York State Department of Transportation. *Concrete Grouting Materials*, 701-05, last accessed April 8, 2016, <https://www.dot.ny.gov/divisions/engineering/technical-services/technical-services-repository/alme/pages/220-1.html>.
49. New York State Department of Transportation. *Cement Based Grout Materials for Shear Keys*, 701-06, last accessed April 8, 2016, <https://www.dot.ny.gov/divisions/engineering/technical-services/technical-services-repository/alme/pages/230-1.html>.
50. ASTM C39/C39M (2015). *Standard Test Method for Compressive Strength of Cylindrical Concrete Specimens*. ASTM International. West Conshohocken, PA.
51. ASTM C579 (2012). *Standard Test Methods for Compressive Strength of Chemical-Resistant Mortars, Grouts, Monolithic Surfacing, and Polymer Concretes*. ASTM International. West Conshohocken, PA.





